ERS-2 Wind Scatterometer Cyclic Report

from 19th November 2001 to 24th December 2001
Cycle 69

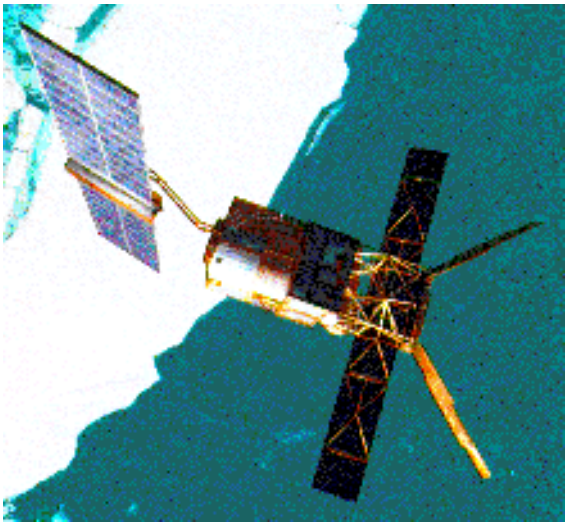

Prepared by:	PCS team	ESRIN EOP-ADQ
Inputs from:	F. Aidt	ESTEC TOS-EMS
	H. Hersbach	ECMWF

Issue:	1.0
Reference:	ERSE-SPPA-EOAD-TN-02-0001
Date of issue:	21st January 2002
Status:	Approved
Document type:	Technical Note
Approved by:	P. Lecomte

Distribution List

(Summary only via e-mail)

ESTEC	M. Canela	EOP-PR
	E. Attema	EOP-FSS
	M. Drinkwater	EOP-FSO
	F. Aidt	TOS-EMS
	B. Gelsthorpe	EOP-PTR
	R. Zobl	EOP-P
	K. van't Klooster	TOS-EEA
ESOC	F. Bosquillon de Frescheville	TOS-OFC
	L. Stefanov	TOS-OFC
ESRIN	M. Albani	EOP-AD
	P. Lecomte	EOP-ADQ
	V. Beruti	EOP-ADF
	S. Jutz	EOP-ADU
	G. Kohlhammer	EOP-AM
	M. Onnestam	EOP-ADC
	G. Emiliani	EOP-ADQ-PCS

L.A. Breivik	DNMI
P. Snoeij	DUT
J. Heidbreder	DORNIER
L. Isaksen, H. Hersbach	ECMWF
J. Kerkman, J. Figa	EUMETSAT
V. Wismann	IFARS
A. Cavanie	IFREMER
R.S. Dunbar	JPL
A. Stoffelen, T. Driessenaar	KNMI
G. Legg, P. Chang	NOAA/NESDIS
W. Gemmill	NOAA/NWS
J. Hawkins	NRL
D. Offiler, R. Graham, C.A. Parrette	UK-MET Office
F. Courtier, H. Roquet	Meteo-France
C. Scupniewicz	FNMOC
R.A. Brown	University of Washington
J. Boutin	LODYC/UPMC
M.A. Messeh	University of Sheffield

This report and its annex (ECMWF report) are available on PCS web:
http://pcswww.esrin.esa.it

1.0 Introduction and summary

The document includes a summary of the daily quality control made within the PCS and various sections describing the results of the investigations and studies of "open-problems" related to the Scatterometer. In each section results are shown from the beginning of the mission in order to see the evolution and to outline possible "seasonal" effects. An explanation for the major events which have impacted the performance since launch is given, and comments about the recent events which occurred during the last cycle are included.

This report covers the period from 19th November 2001 to 24th December 2001(cycle 69).

It contains a new chapter with the results of the estimation of the yaw error angle by using Scatterometer raw data. In the actual Zero Gyro (ZGM) configuration the main problem in the satellite attitude is really the piloting around the Z-Axis used to minimize the Doppler frequency in the received signal. The estimation of the yaw error angle is a fundamental step in the new Ers Scatterometer Attitude Corrected Algorithm (ESACA) under development by ESA.

The PCS at ESRIN had developed a prototype for a coarse estimation of the yaw error angle. Details regarding the algorithm used are available in the Technical note " Impact of a yaw error angle in the Scatterometer Doppler Frequency". The study carried out in ESRIN shows that the main problem in the yaw estimation is the received signal bandwidth that is limited by the on-board low pass filter. As consequence only small yaw angle (within +/- 3 deg) can be estimated. The prototype developed in ESRIN has been tested against the SAR wave yaw angle estimator also developed in ESRIN. The result is a good agreement between the two methods in particular for small error angles.

The coarse yaw estimator was used to asses the yaw performances since the beginning of the ZGM commissioning (June 2001). During the last 6 months the orbits that had passed the quality control (standard deviation less than 1 deg. and with an absolute bias below 3 deg.) were roughly 40%. That result is mainly due to the tuning of the AOCS parameters throughout June 2001 and strong solar activity in October and November 2001 that further degraded the satellite attitude.

For the cycle 69 the result is more encouraging: the orbits that had passed the quality control were roughly 75%. It is foreseen that for those orbit ESACA will be able to retrieve calibrated sigma noughts.

Mission events

- During the cycle 69 the ERS-2 satellite was still in ZGM commissioning phase. No new tuning of the onboard parameters were performed for that cycle.
- ERS-2 payload was switched-off from 27th November 2001 to 28th November 2001 due to the Mono-Gyro Coarse Mode Commissioning.
- As mentioned in the previous report, peaks in the solar activity have a negative impact in the satellite attitude. During the cycle 69 a yaw degradation was recorded on days 3rd, 24th November, 12thand 24th December 2001 (see http://umtof.umd.edu/pm/FIGS.HTML).
- The AMI instrument was still operated in wind-wave mode throughout the whole orbit. This mode allow to estimate yaw error angle along the orbit by analysing the SAR imagette.
- During the cycle 69 no Scatterometer products were disseminated to the users.

- The PCS continues its mission monitoring and results are given in the following paragraphs.

Calibration performance

- The calibration performances show an improvement with reference to cycle 68. The reason is a more stable attitude of the platform during the cycle 69. Of course sigma nought are not yet calibrated but their variation over the Rain Forest show a reduction. The amplitude of the Gamma nought variation, over the test site, during the cycle 69 was roughly 2.5 dB (10 dB for the previous cycle).
- The shape of the antenna pattern are fairly different if compared with cycle 68. In particular during the cycle 69 the dependency of the gamma nought wrt the incidence angle for the Mid and Fore antenna was reduced and the antenna profiles became more flat. On the other hand, the Aft antenna shows a more flat pattern only for an incidence angle ranging between 25 and 40 degrees and a clear slope above 40 degrees. The result is a near range - far range difference within 0.5 dB for the Mid and Fore antenna (2.0 dB during cycle 68) and still 2.0 dB (as for cycle 68) for the Aft antenna. Those 2.0 dB are mainly due to the slope present in the antenna pattern above 40 degrees incidence angle. Moreover for low incidence angle the Aft beam signal is roughly 0.5 dB above the Fore/Mid signal. That result is in agreement with the Ocean Calibration performed by ECMWF but puts on the table interesting questions. First of all the degradation of the sigma noughts reported for the previous cycles was roughly linear wrt the incidence angle. That behaviour was nominal and coherent with the degradation introduced with the yaw error angle. In that case the linear degradation is only above 40 degrees for the Aft beam. The second point regards the different behaviour among the three antennae. If for a small region as the test area is easy to assume that the satellite attitude change during the acquisition (we have roughly 200 sec of difference between the Fore and Aft sensing time over the same area) the same reason cannot be addressed for the Ocean monitoring that covers the entire globe. A preliminary conclusion is that the degradation of the Aft antenna pattern could be due to the antenna itself (e.g. thermal protection ageing) rather than problem in satellite attitude. The antenna patterns are under constant monitoring by the PCS and a better analysis shall be provided in the next reports.
- During the calibration passes of the cycle 69 the Transponders were working nominally but the CALPROC system is not able to process any more the data acquired in ZGM: the results are meaningless. For that reason new gain constant will not available until a new version of CALPROC is implemented.

Instrument performance

- The power decrease was on average 0.15 dB/cycle. The actual level of the transmitted power is roughly 0.83 dB below the level reached in October 1998 and therefore a new power increase shall be agreed with ESOC.
- The Doppler frequency monitoring confirms the degradation of the satellite attitude due to solar activity on days 3rd, 24th November, 12thand 24th December 2001. On average the CoG of the received spectrum is roughly 1.5KHz for the Aft and Fore beam and roughly 500Hz for the Mid beam. The CoG standard deviation is roughly 4.5 Khz for the Fore and Aft beam and 5.3 KHz for the Mid beam.
- The monitoring of the noise power shows a stable result.

- The monitoring of the antennae temperature over the Brazilian Rain Forest shows a stable evolution during the cycle 69. It confirms the temperature increase of 1 deg/year for the Fore and Mid Antenna and roughly 2 deg/year for the Aft antenna.

Product performance

- During the cycle 69 the wind speed bias (UWI vs ECMWF forecast) stayed stable around 0.3 m/s. The wind speed standard deviation was around 3 m/s. The number of valid nodes per day was roughly 180000.

2.0 Calibration Performances

The calibration performances are estimated using three types of target: a man made target (the transponder) and two natural targets (the rain forest and the ocean). This approach allow us to design the correct calibration using a punctual but accurate information from transponders and an extended but noisy information from rain forest and ocean for which the main component of the variance comes from the geophysical evolution of the natural target and from the backscattering models used. These aspects are in the calibration performance monitoring philosophy. The major goals of the calibration monitoring activities are the achievement of a “flat” antenna pattern profile and the assurance of a stable absolute calibration level.

2.1 Gain Constant over transponder

One gain constant is computed per transponder per beam from the actual and simulated two-dimensional echo power, which is given as a function of the orbit time and range time. This parameter clearly indicates the difference between “real instrument” and the mathematic model. In order to acquire data over the transponder the Scatterometer must be set in an appropriate operational mode defined as “Calibration Mode”.

Table 1 shows the result of the calibration plan for cycle 69 The “Yes” in the EWIC column means that the raw data are available, “No” means that some problems caused a loss of data. The “On” in the transponder status column means that, from the raw data (EWIC), the transponders have been recognised as switched-on; “Off” that they were off. The “Yes” in the GC computed column means that a gain constant value has been retrieved, “No” means the opposite case. As reported in Table 1 the calibration plan, during the cycle 69 was executed as planned but due to the degraded attitude the calibration data are meaningless. For that reason no new gain constant will be available until a new version of CALPROC is implemented. Furthermore it is not even possible, from the received data, to recognise if the transponder was switched on or not.

TABLE 1. Calibration Plan: cycle 69

DATE	ORBIT (absolute)	ORBIT (relative)	Passage	Ground Station	EWIC (raw data)	AMI mode	Transponder Status	GC computed
011120	34431	8	D	KS	Yes	Calibration	n/a	n/a
011123	34474	51	D	KS	Yes	Calibration	n/a	n/a
011208	34693	273	A	MS	Yes	Calibration	n/a	n/a
011211	34739	316	A	MS	Yes	Calibration	n/a	n/a

Figure 1 and Figure 2 show the valid gain constants available **since the beginning of the mission until cycle 60 (end of mono-gyro operation)**. The analysis is made for various antenna elevation angle. From these figures it is clear that the gain constant measurements are stable (within +/-0.5 dB).

The plots in Figure 3 show the value of the Gain Constant for the three beams and for the ascending, descending and all passes. The plots show the average of all gain constants available since January 1996 (cycle 8) for each antenna elevation angle. The antenna patterns are flat but there is a clear shift of the level of the curves. On average, the mid beam is 0.3 dB higher than the aft one

and 0.5 dB higher than the fore one. For the descending passes the antenna pattern shows a slight negative slope from far range to near range.

Since September 1996, ESTEC has added a scaling factor to the gain constant in order to remove the bias among the three antennae. The gain constants were increased by 0.2 dB, -0.3 dB and 0.2 dB, for the fore, mid and aft beam respectively. The result is shown in Figure 4. The suggestion given by ESTEC has not been introduced into the ground processing because the antenna patterns computed over the rain forest do not show such bias (see Figure 5 in the cyclic report before cycle 60 during the nominal YSM). So in the actual scenario, the differences among the antennae are considered as a bias due to the transponder themselves.

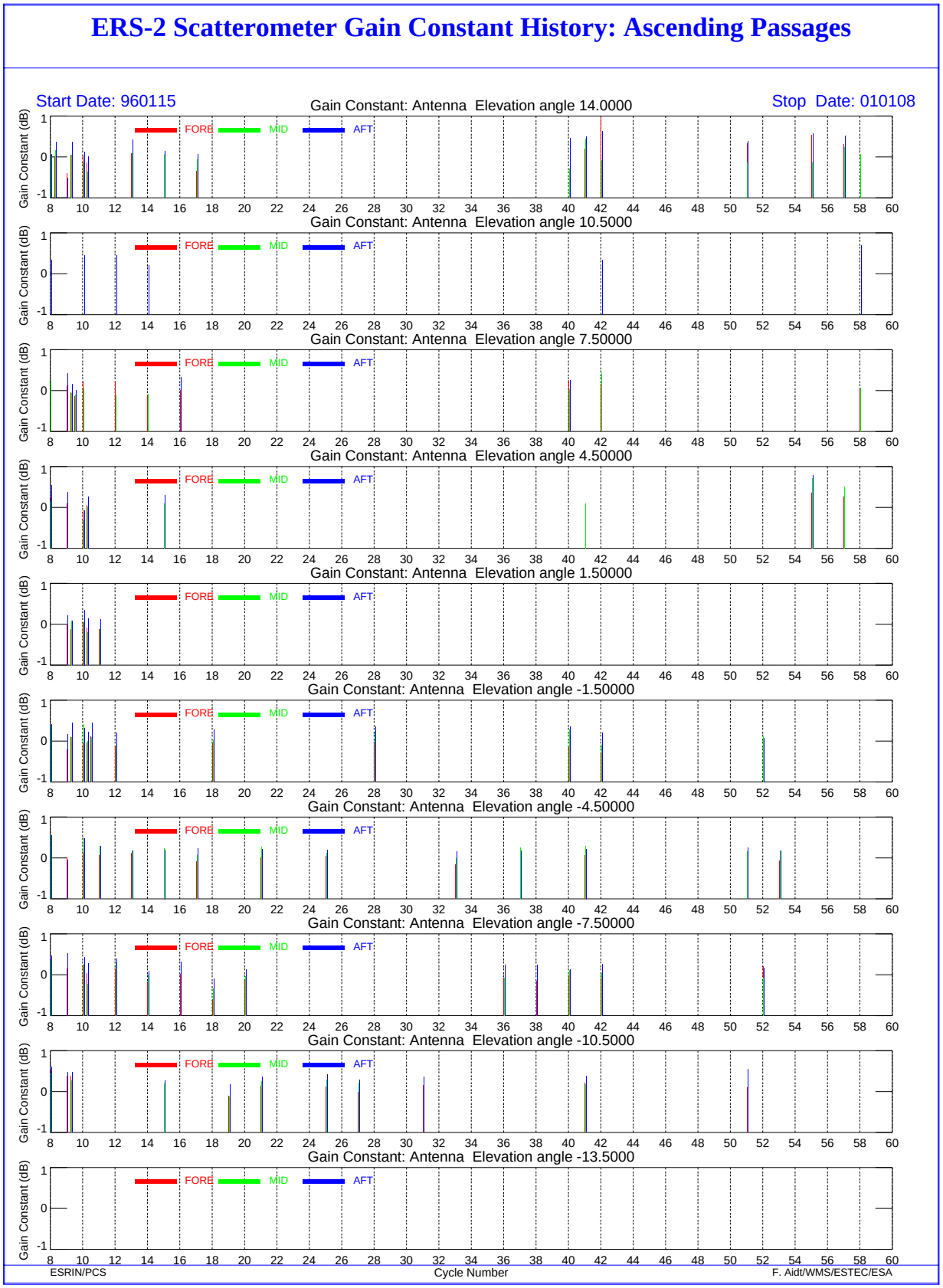

FIGURE 1. ERS-2 Scatterometer; gain Constant over transponder since the beginning of the mission until cycle 60 (ascending passes).

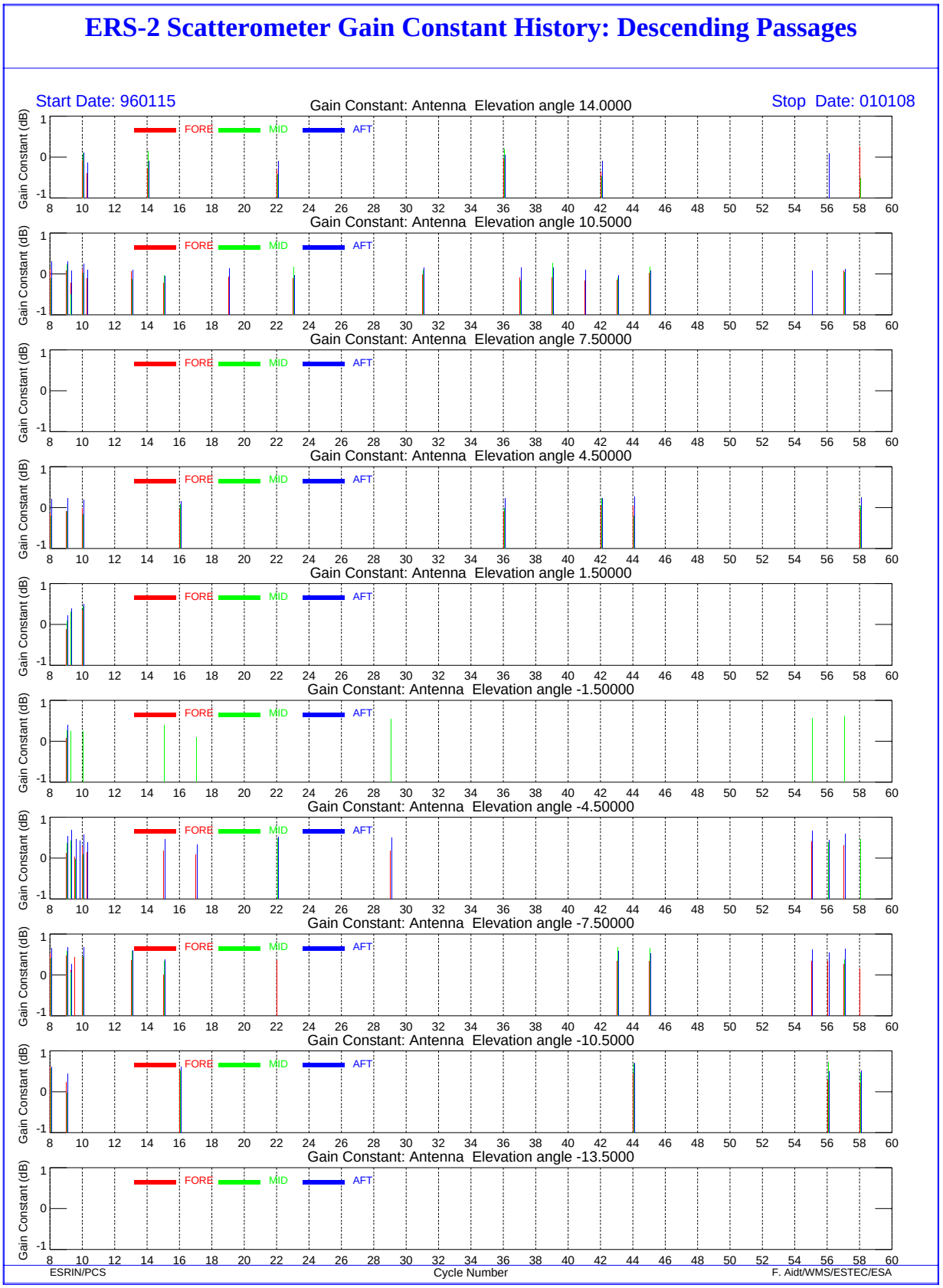

FIGURE 2. Scatterometer; gain Constant over transponder since the beginning of the mission until cycle 60 (descending passes)

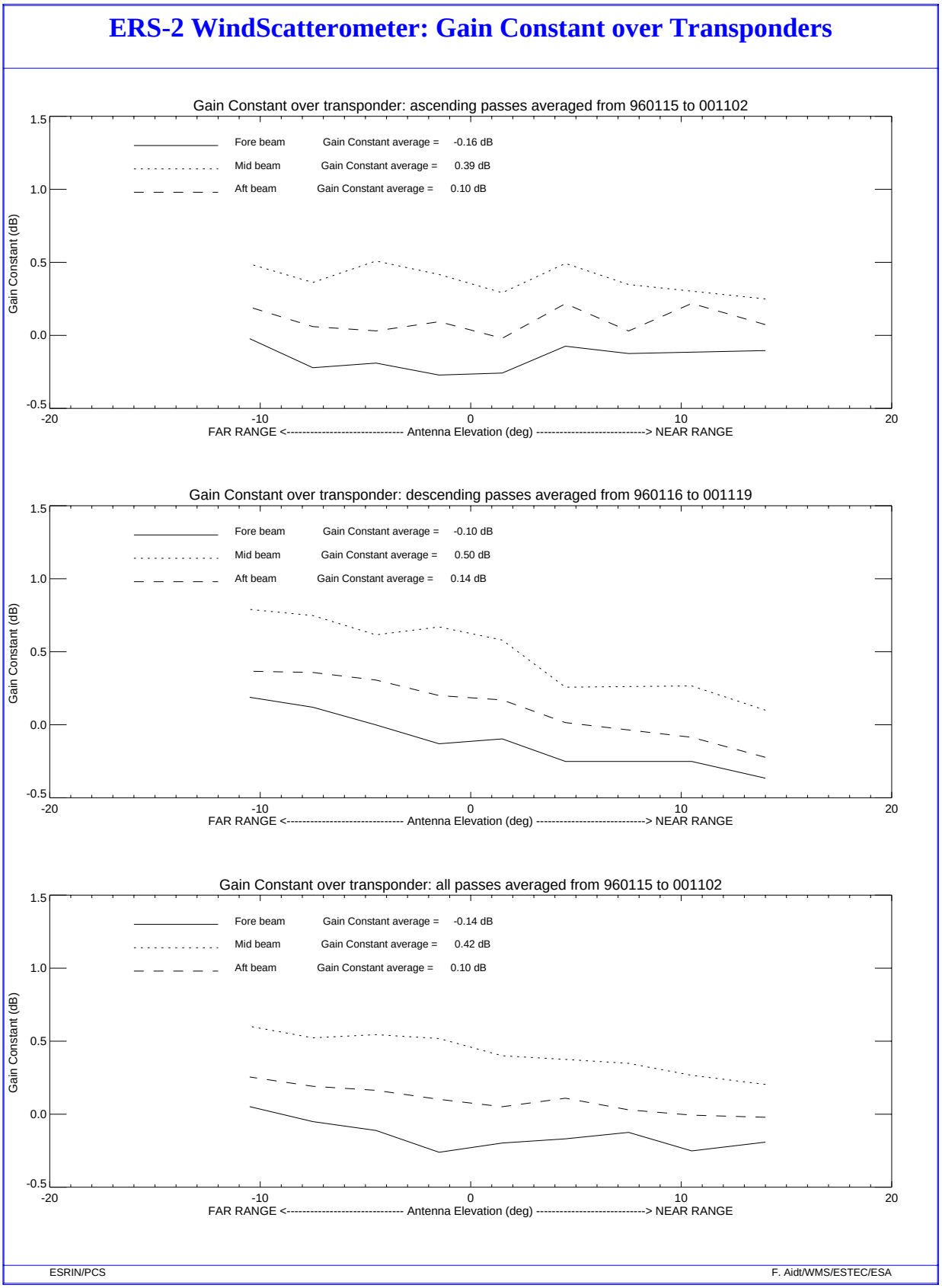

FIGURE 3. ERS-2 Scatterometer: gain constant over transponders. All data available since January 1996 until cycle 60. Upper plot: ascending passes. Middle plot: descending passes. Lower plot: all passes.

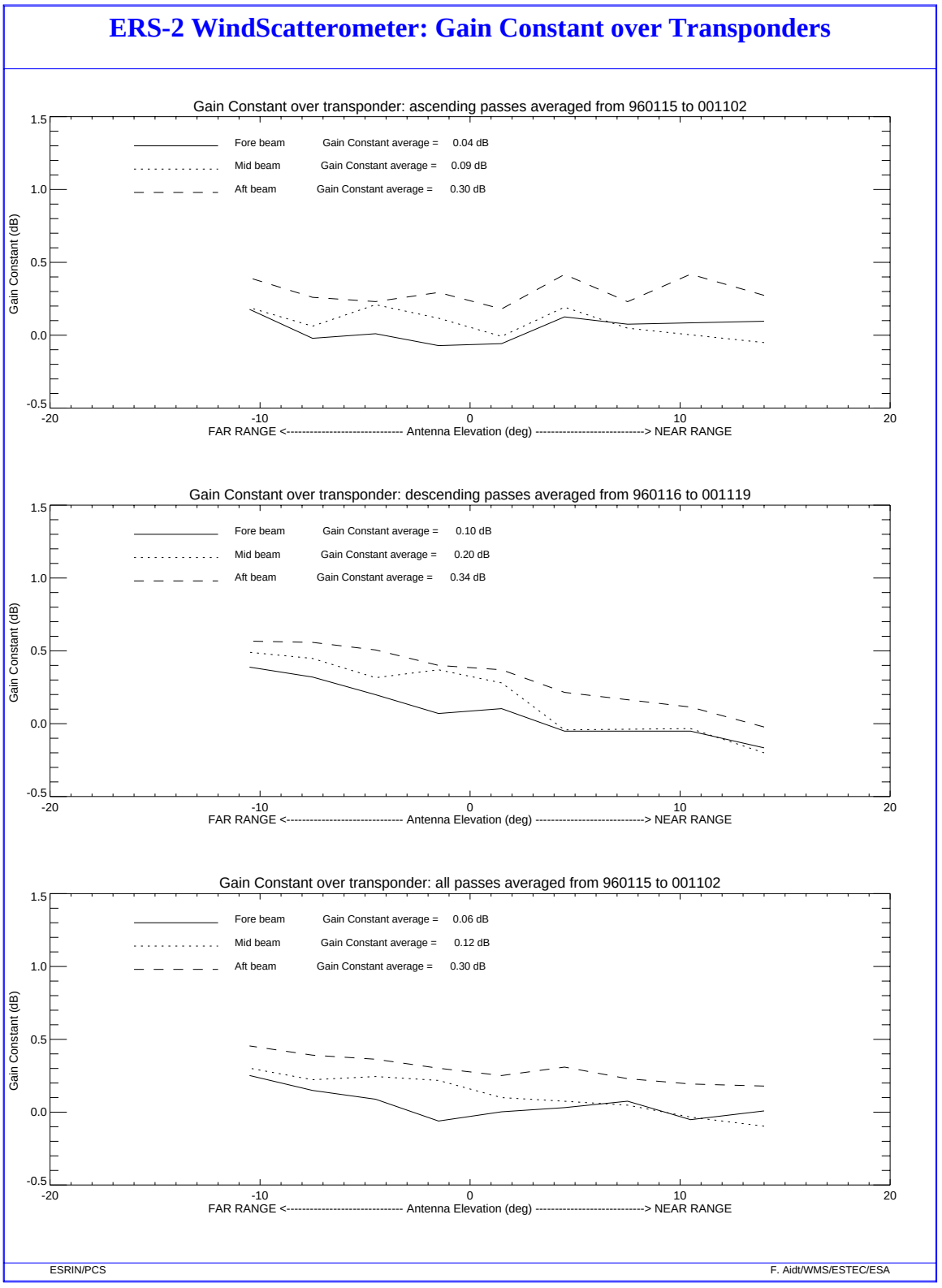

FIGURE 4. ERS-2 Scatterometer: gain constant over transponders plus a scaling factor. All data available since January 1996 until cycle 60). Upper plot: ascending passes. Middle plot: descending passes. Lower plot: all passes.

2.2 Ocean Calibration

During the cycle 69 (from 12th December 2001 onwards) Scatterometer data were disseminated to ECMWF for monitoring purpose.

The Scatterometer sigma noughts were compared with the ECMWF model first guess winds. The analysis was done for each incidence angle both ascending and descending passes.

The result was a large negative bias. For the Mid antenna that bias was independent from the incidence angle while for the Aft and Fore there was a correlation between the sigma bias and the incidence angle. The shape of the antenna pattern provided by ECMWF is very similar to the one obtained by PCS over the Rain Forest (see Figure 5 on section 2.3.2).

Further comments are in section 2.3.2

2.3 Gamma-nought over Brazilian rain forest

Although the transponders give accurate measurements of the antenna attenuation at particular points of the antenna pattern, they are not adequate for fine tuning across all incidence angles, as there are simply not enough samples. The tropical rain forest in South America has been used as a reference distributed target. The target at the working frequency (C-band) of ERS-2 Scatterometer acts as a very rough surface, and the transmitted signal is equally scattered in all directions (the target is assumed to follow the isotropic approximation). Consequently, for the angle of incidence used by ERS-2 Scatterometer, the normalised backscattering coefficient (sigma nought) will depend solely on the surface effectively seen by the instrument:

$$S^0 = S \bullet \cos\theta$$

With this hypothesis it is possible to define the following formula:

$$\gamma^0 = \frac{\sigma^0}{\cos\theta}$$

Using this relation, the gamma nought backscattering coefficient over the rain forest is independent of the incident angle, allowing the measurements from each of the three beams to be compared.

The test area used by the PCS is located between 2.5 degrees North and 5.0 degrees South in latitude and 60.5 degrees West and 70.0 degrees West in longitude.

The following paragraphs give a description of the activities carried out with this natural target.

2.3.1 Antenna pattern: Gamma-nought as a function of elevation angle

This analysis is normally carried out by ESTEC which has selected a larger region than the one used as test area by the PCS. In this case the selected rain forest extends from 2.0 degrees South to 11.0 degrees South in latitude and 56.0 degrees West to 80 degrees West in longitude. This large area was selected in order to increase the number of measurements.

For cycle 69, the antenna patterns in function of the elevation angle have not been computed by ESTEC.

2.3.2 Antenna pattern: Gamma-nought as a function of incidence angle

Figure 5 shows the antenna patterns as a function of the incidence angle for cycle 69.

The shape of the antenna pattern are fairly different if compared with cycle 68. In particular during the cycle 69 the dependency of the gamma nought wrt the incidence angle for the Mid and Fore antenna was reduced and the antenna profiles became more flat. On the other hand, the Aft antenna shows a more flat pattern for an incidence angle ranging between 25 and 40 degrees and a clear slope above 40 degrees.

The result is a near range - far range difference within 0.5 dB for the Mid and Fore antenna (2 dB during cycle 68) and still 2 dB (as for cycle 68) for the Aft antenna. Those 2 dB are mainly due to the slope present in the antenna pattern above 40 degrees incidence angle.

That result is in agreement with the Ocean Calibration but puts on the table interesting questions. First of all the degradation of the sigma noughts reported for the previous cycles was roughly linear wrt the incidence angle. In that case the linear degradation is only above 40 degrees for the Aft beam.

The second point regards the different behaviour among the three antennae. If for a small region as the test area is easy to assume that the satellite attitude change during the acquisition (we have roughly 200 sec of difference between the Fore and Aft sensing time over the same area) the same reason cannot be addressed for the Ocean monitoring that covers the entire globe.

A preliminary conclusion is that the degradation of the Aft antenna pattern could be due to the antenna itself (e.g. thermal protection ageing) rather than problem in satellite attitude. The antenna patterns are under constant monitoring by the PCS and a better analysis shall be provided in the next reports.

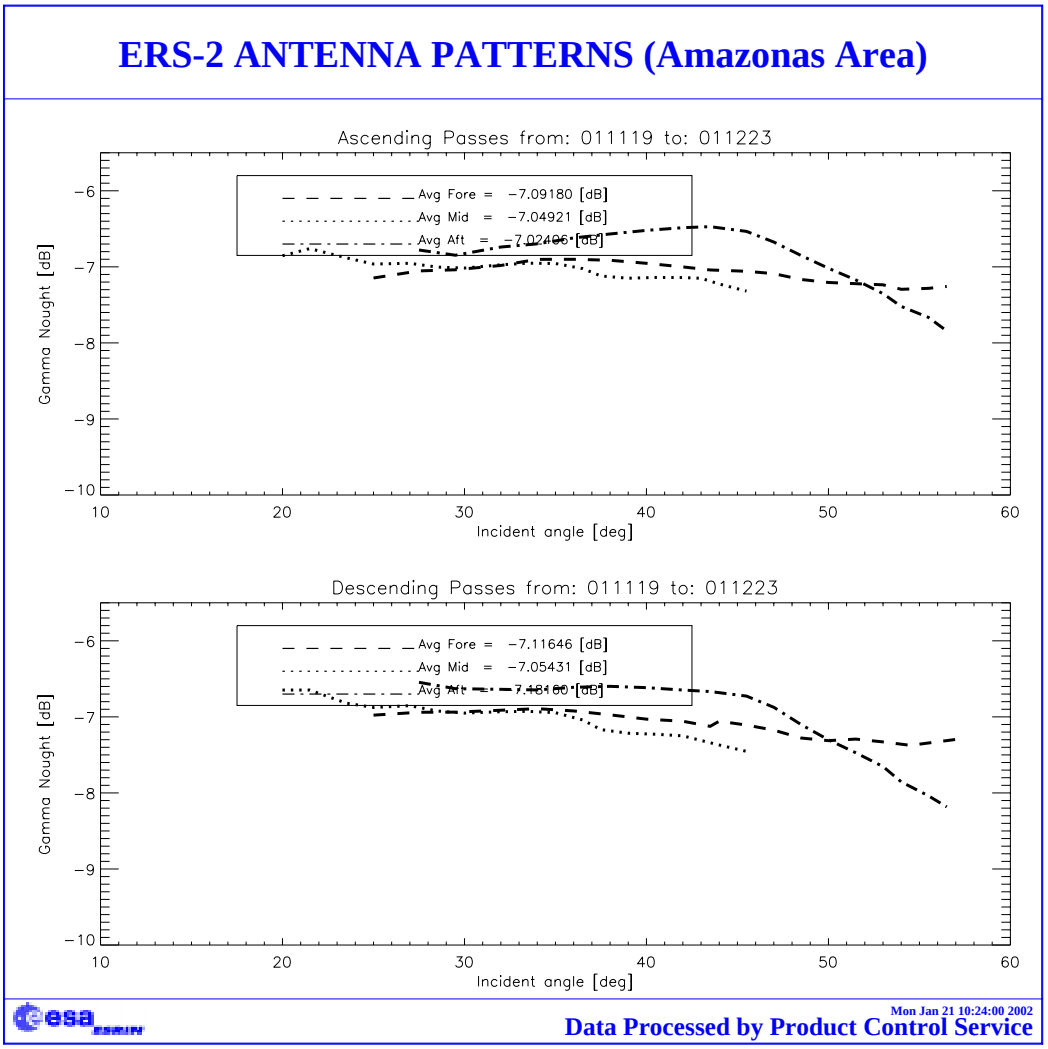

FIGURE 5. ERS-2 Scatterometer antenna patterns as function of the incidence angle: cycle 69.

2.3.3 Gamma nought histograms and peak position evolution

As the gamma nought is independent from the incidence angle, the histogram of gamma noughts over the rain forest is characterised by a sharp peak. The time-series of the peak position gives some information on the stability of the calibration. This parameter is computed by fitting the histogram with a normal distribution added to a second order polynomial:

$$F\langle x\rangle = A_0 \cdot \exp\left(-\frac{z^2}{2}\right) + A_3 + A_4 \cdot x + A_5 \cdot x^2$$

where: $$z = \frac{x - A_1}{A_2}$$

The parameters are computed using a non linear least square method called “gradient expansion”. The position of the peak is given by the maximum of the function F(x). The histograms are computed weekly (from Monday to Sunday) for each antenna individually (“Fore”, “Mid”, and “Aft”) and for ascending and descending passes with a bin size of 0.02 dB.

Figure 6 shows the evolution of the histograms peak position since January 1996. The step shown in March 1996 is due to the end of commissioning phase when a new Look Up Table was used in the ground stations for WSCATT FD-products generation. It is interesting to note the decrease of roughly 0.2 dB from August 1996 to June 1997. This is linked to the switch of the Scatterometer calibration subsystem from side A to side B on 6th of August. The redundancy of side A device caused a little change in the calibration that was corrected on 19th June 1997 with a new calibration LUT used in the ground processing.

Figure 7 shows the evolution of the peak position corrected with the new calibration set also for the period from August 1996 to June 1997. The plots in Figure 7 show that the calibration stability achieved over the rain forest is within 0.5 dB. A seasonal effect is also present in the peak position evolution for the three antennae.

After the 17th January 2001 a meaning full monitoring of the peak position is not possible any more. Due to satellite degraded attitude the signal from Rain Forest is not stable, and the histograms’ shape (see figures from 10 to 14) does not show a sharp peak. This explains the high fluctuation in the time series from January 2001 onwards.

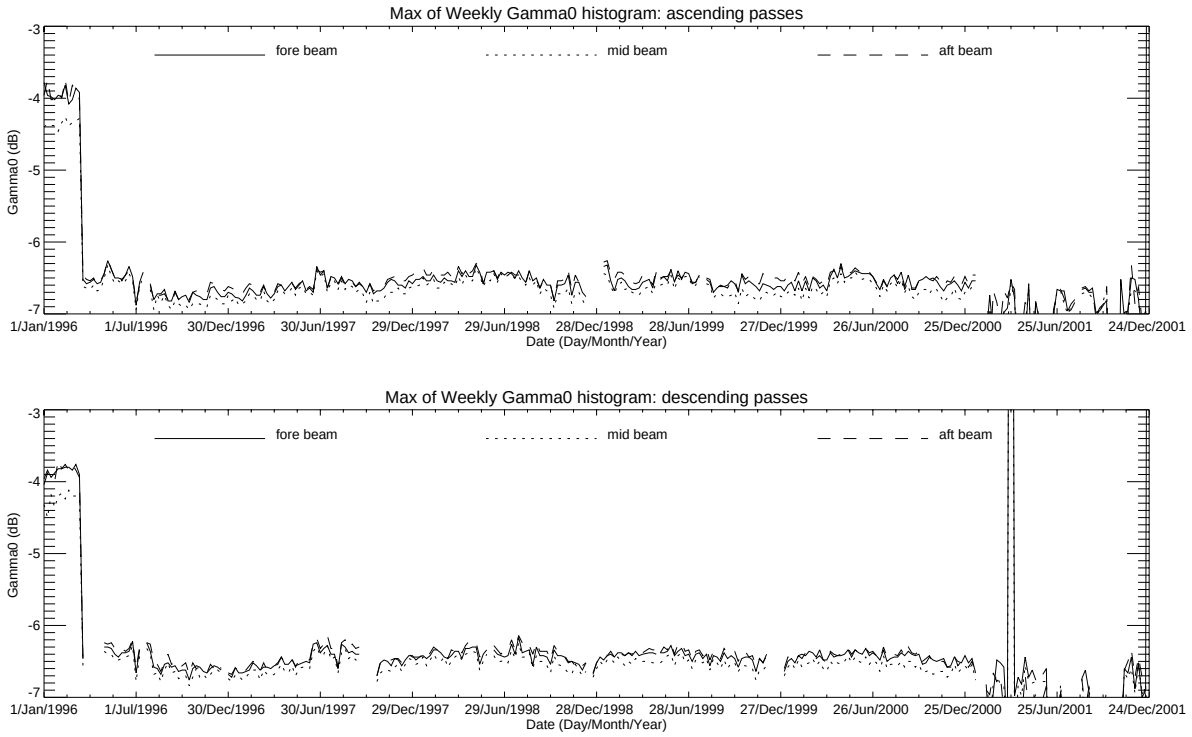

FIGURE 6. ERS-2 Scatterometer, gamma-nought histogram: weekly evolution of maximum position. From up to down: ascending passes, descending passes.

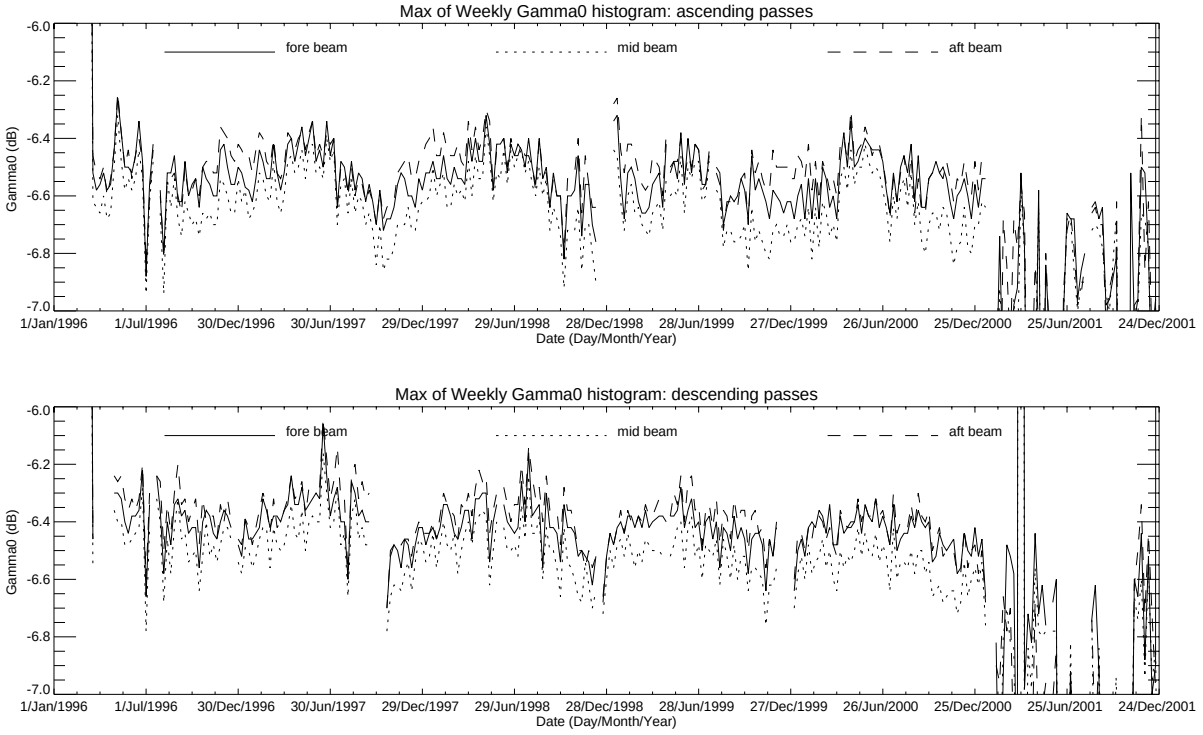

FIGURE 7. Gamma-nought histogram: weekly evolution of maximum position. Data from 6th of August 1996 to 19th June 1997 are corrected with the new calibration constant (+0.2dB). Upper plot: ascending passes. Lower plot: descending passes.

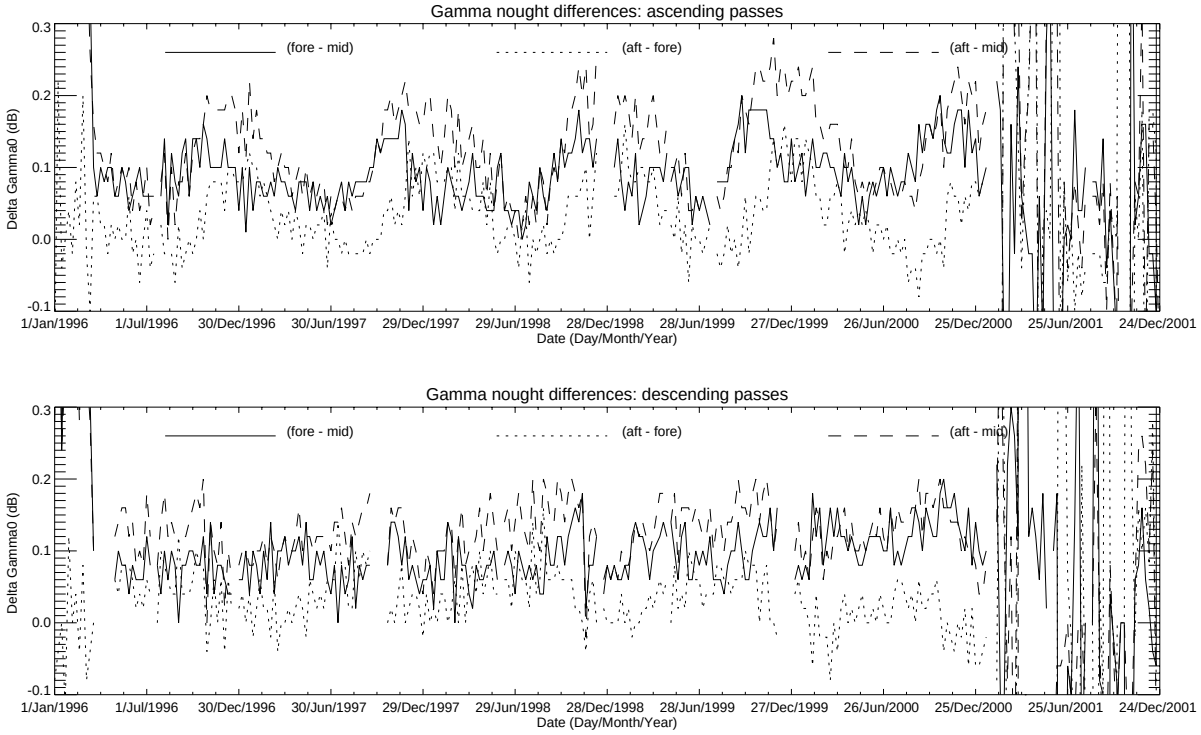

FIGURE 8. Inter-beam calibration, weekly differences of the maximum position since 1st January 1996. From up to down: ascending passes, descending passes.

For the inter-beam calibration, the results since 1996 are shown in Figure 8.

For the ascending passes, the differences in the signals have a seasonal behaviour. On average the differences are close to 0.1 dB during the summer and they are close to 0.2 dB during the winter. For the descending passes, the differences between the winter and the summer are less clear and the inter-beam calibration is around 0.1 dB (-0.03 dB for the aft-fore signal during the cycle 59).

A change around the end of year 1999 and the beginning of year 2000 is clearly present in the (aft-fore) difference signal as well as in the (aft-mid) signal. Investigations have been carried out in order to recognize which antenna has caused the change in the inter-beam calibration (see the report for the cycle 53). It can be noted that this evolution has mainly affected the Aft antenna with a mean decrease of roughly 0.05 dB in the signal. Because of the noise in the time series, it is also difficult to estimate if this evolution is related to mission or instrument events. The most relevant mission events were: the payload switch-off to face out the Leonid meteorite shower (November 1999), a series of AMI emergency switch down anomalies and the AOCS mono-gyro configuration (February 2000).

The mean and the standard deviation of the gamma-noughts are weekly computed directly using the Fast Delivery data. Figure 9 shows the evolution of the standard deviation since September 1996. The ascending passes show a gamma nought standard deviation higher than the descending ones. This can be explained because at ascending passes the test site appears less homogeneous; in particular for some areas near the rivers (see gamma nought images before cycle 60). The last plot in Figure 9 shows the number of valid measurements used to compute the statistics.

The high values of the gamma nought standard deviations during the cycle 69 are due to data acquired during the ZGM commissioning phase (see section 3.1).

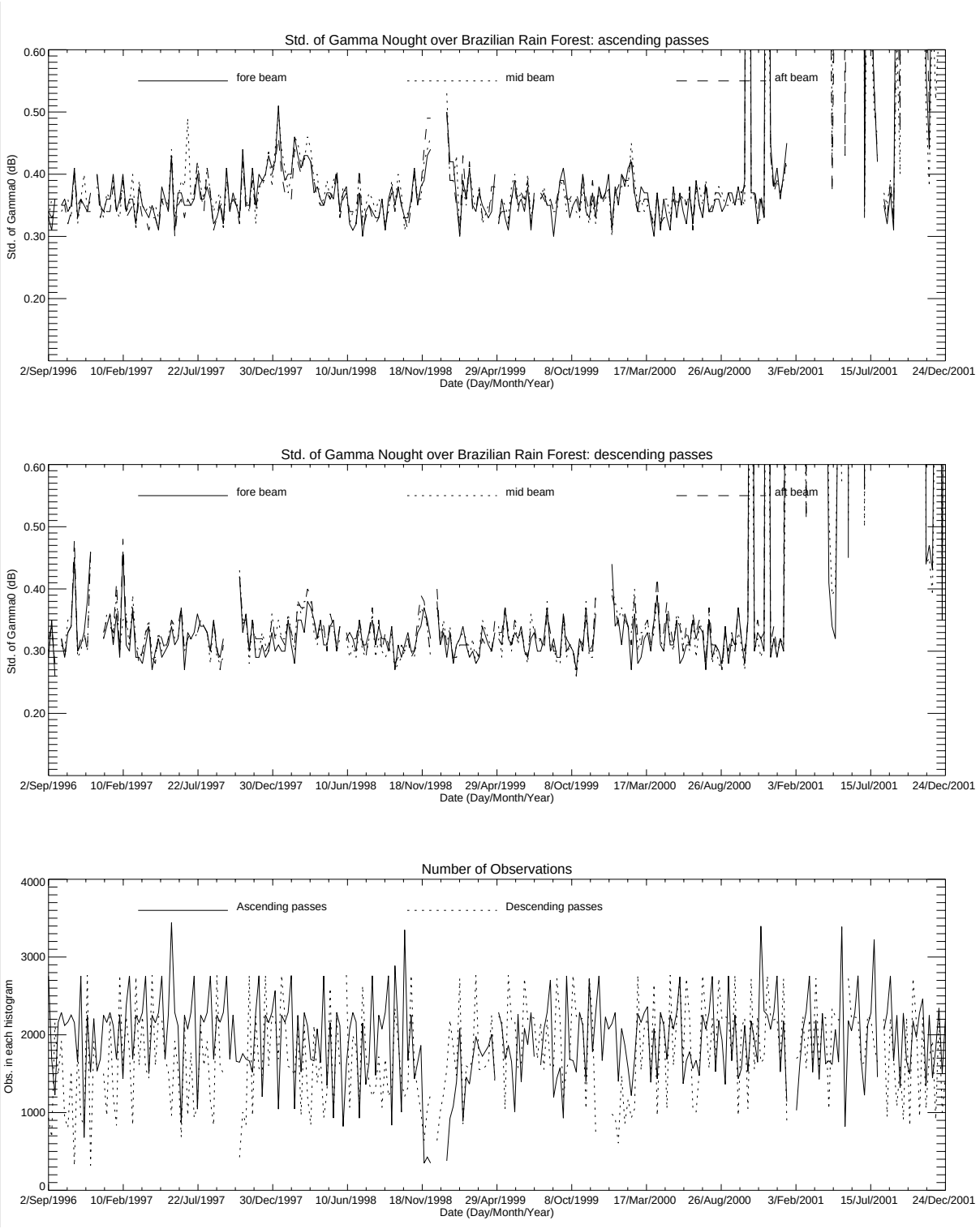

FIGURE 9. Gamma-nought histograms: weekly evolution of standard deviation. From up to down: ascending passes standard deviation, descending passes standard deviation, number of valid observations.

The Figures from 10 to 14 show the gamma nought histogram over the Brazilian rain forest throughout cycle 69.

The histograms for the cycle 69 show in general a bad quality due to the strong degradation of satellite attitude. It is interesting to note (e.g.for week 5) the difference in the histogram's shape for the Fore and Aft antenna over the same area. That difference is due to a change in the satellite attitude during the sensing time.

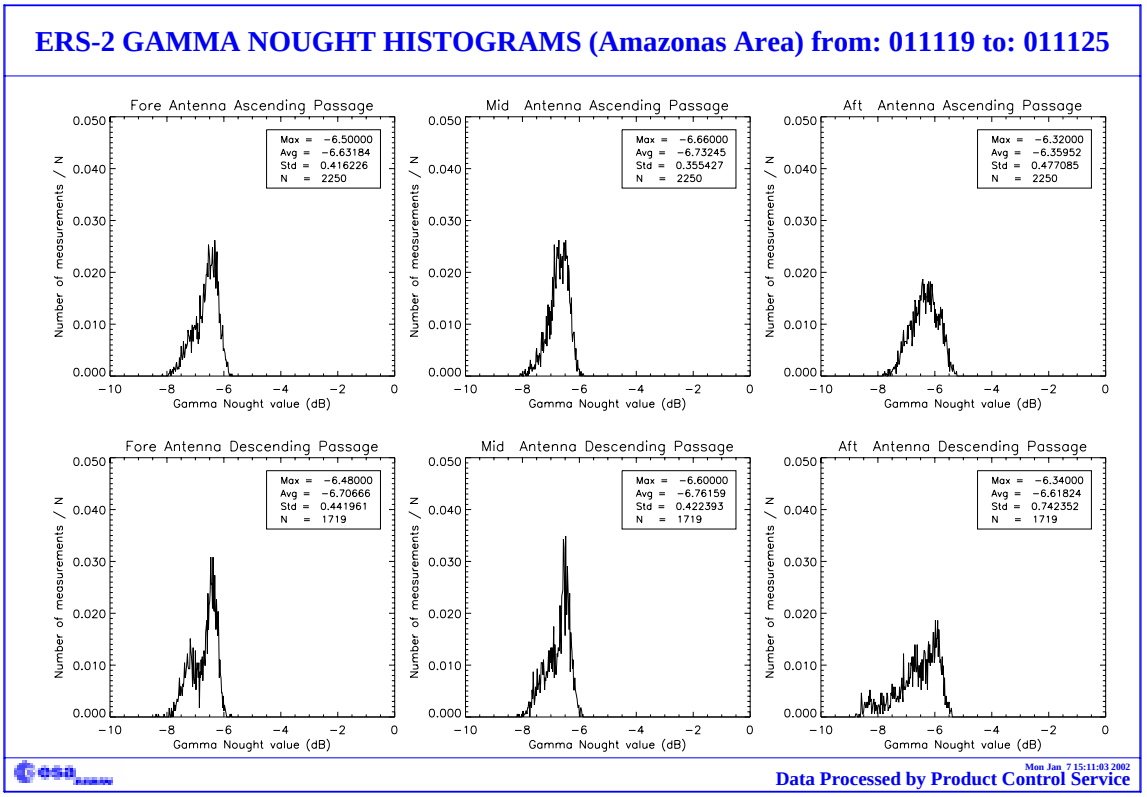

FIGURE 10. Gamma-nought histograms over Brazilian Rain forest: first week of the cycle 69.

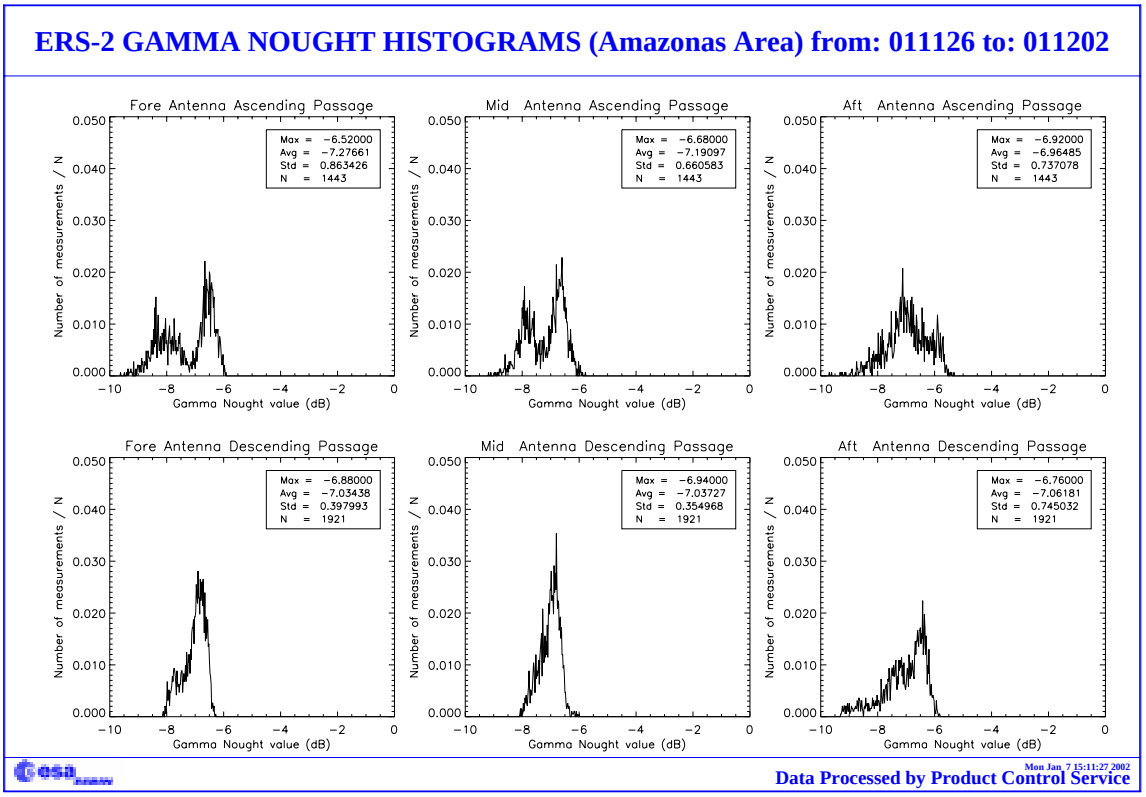

FIGURE 11. Gamma-nought histograms over Brazilian Rain forest: second week of the cycle 69.

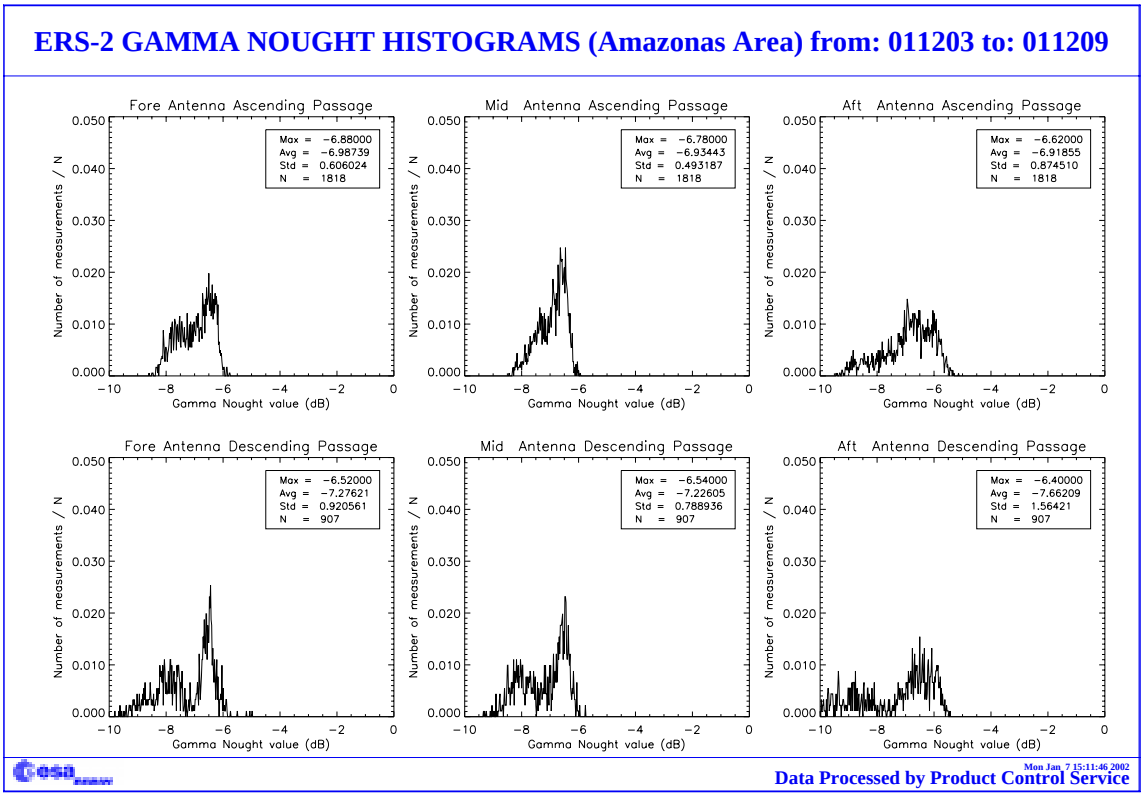

FIGURE 12. Gamma-nought histograms over Brazilian rain forest: third week of the cycle 69.

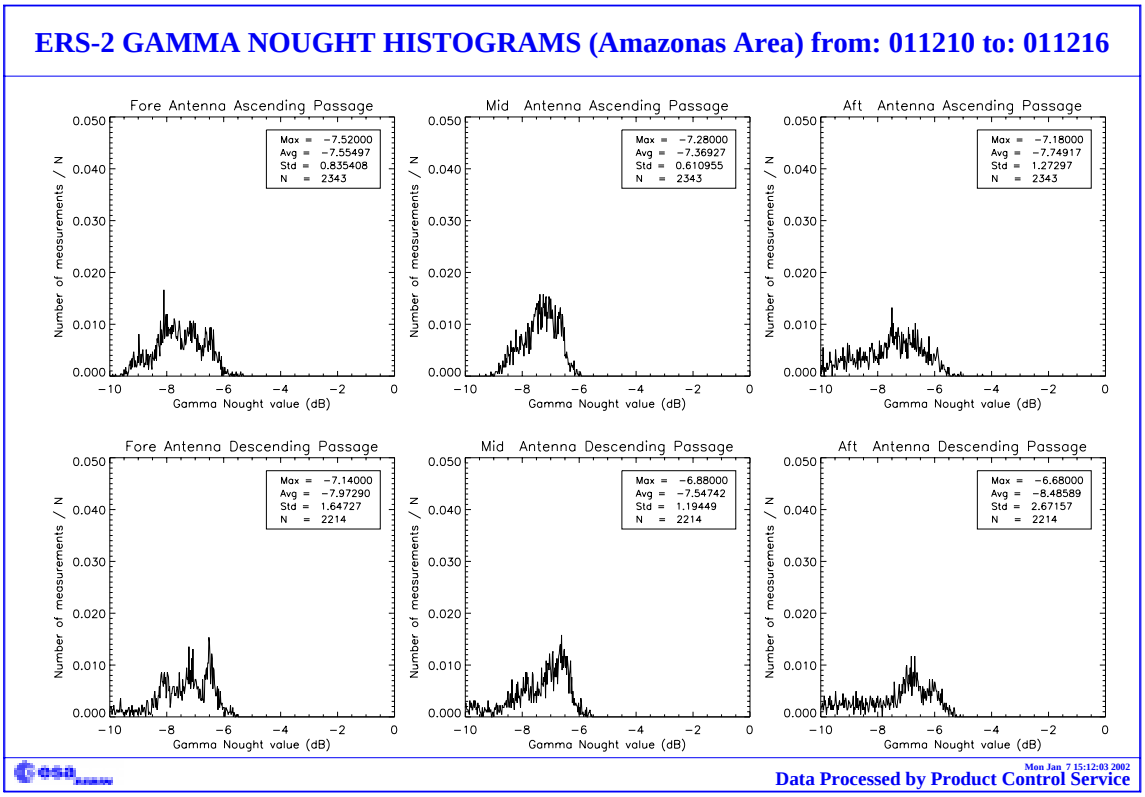

FIGURE 13. Gamma-nought histograms over Brazilian rain forest: fourth week of the cycle 69.

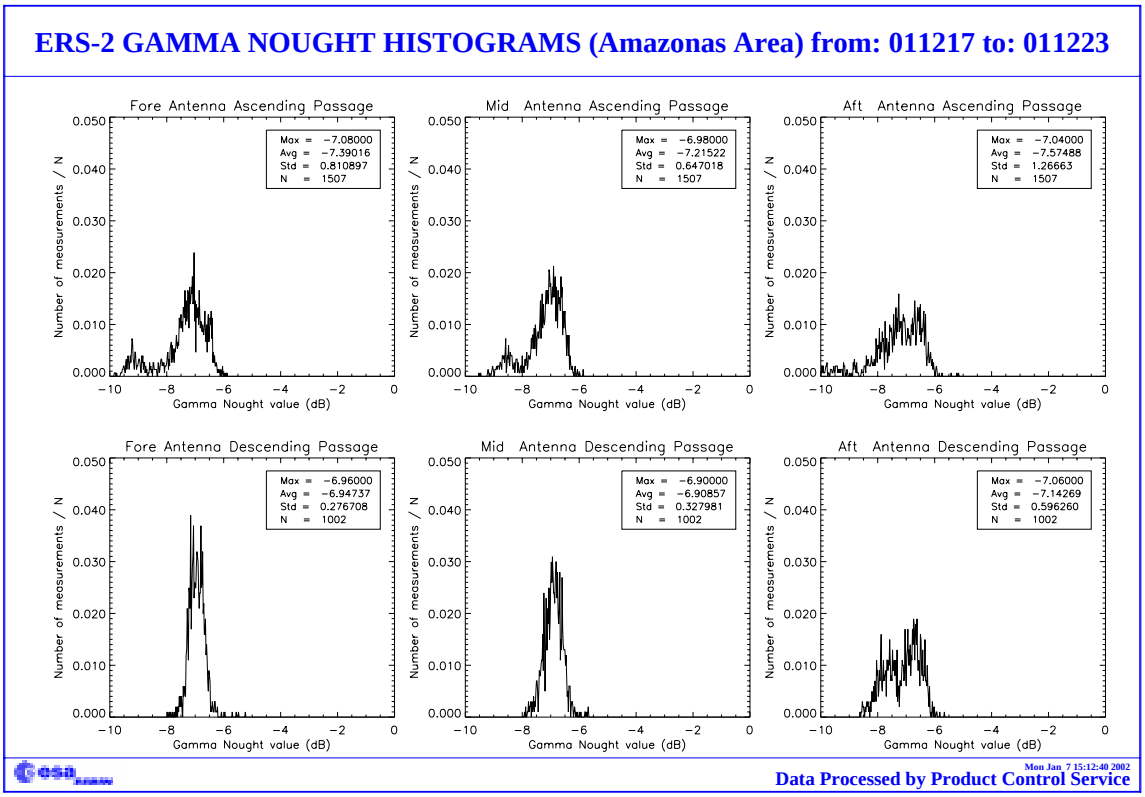

FIGURE 14. Gamma-nought histograms over Brazilian rain forest: fifth week of the cycle 69

2.3.4 Gamma nought image of the reference area

Figure15 shows maps of the gamma nought over the Brazilian rain forest. This is the area where statistics are computed. Each map has a resolution of 0.5 degrees in latitude and 0.5 degrees in longitude, roughly this is the instrument resolution at the latitude of the test site. In each resolution cell falls the average of all the valid observations available during one cycle (35 days).

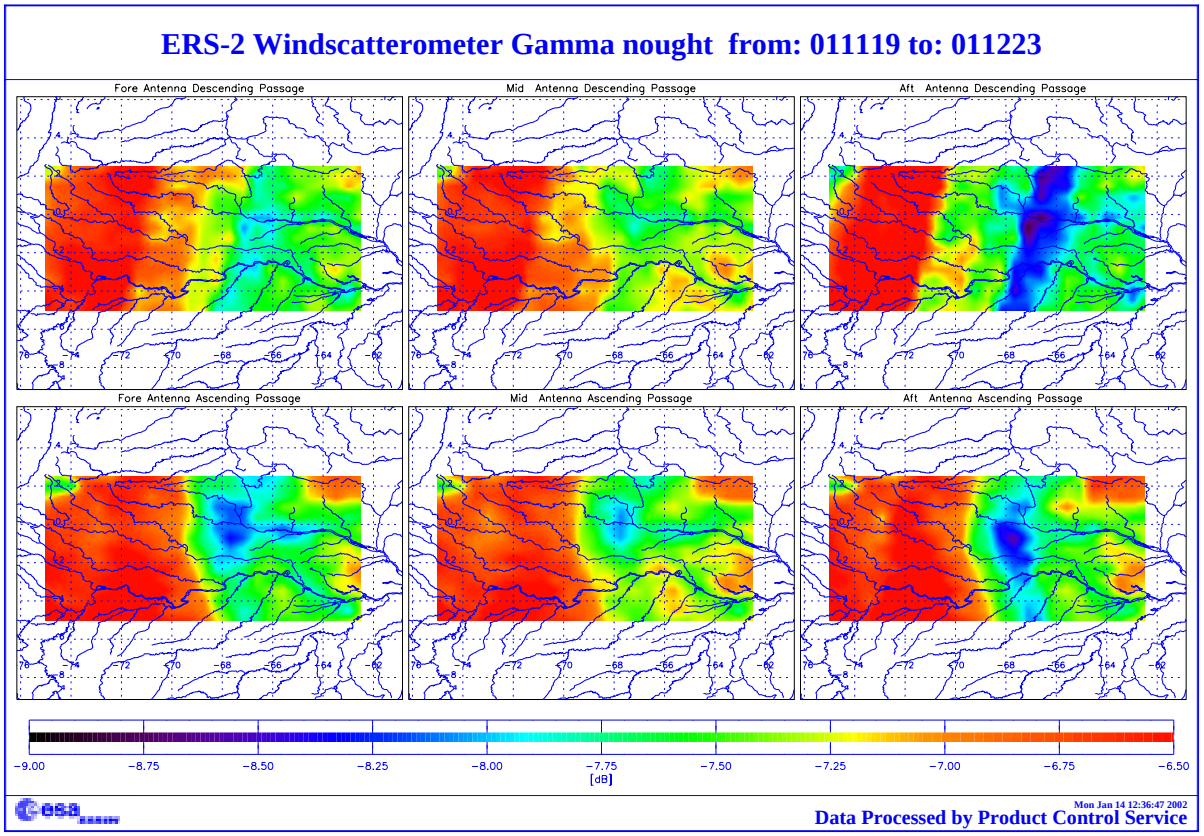

FIGURE 15. ERS-2 Scatterometer: gamma nought over the Brazilian rain forest cycle 69.

Due to degraded satellite attitude the signal over the Rain Forest has a large fluctuation (see the histograms in the previous pages). During the cycle 69 that fluctuation was reduced and **for that reason the colour scale of the image has been fixed from -9 dB to -6.5 dB**. The large differences in the backscattering are due to different satellite attitude among the various passes over the test area.

2.3.5 Sigma nought evolution

The Figures 16 and 17 show the evolution of the sigma nought over the reference area. The analysis is done per orbit and per node and the scope is to evaluate the stability of the sigma nought for each incidence angle. The relative tracks chosen are those where the number of valid measurements for each node (across track) is greater than 20.

The time series show a good correlation among the adjacent nodes (near and far range) and the stability, of the sigma nought, until 17th January 2001, ranges from 0.2 to 0.5 dB depending on the node.

After 17th January 2001 due to operations in EBM mode and ZGM commissioning phase the curves show a clear instability.

For the cycle 69 the improvement in the satellite attitude is clear in the sigma noughts evolution. The Fore and Mid antenna measurements are roughly 1 dB below the nominal one. The analysis for the Aft antenna shows that for the near range the sigma nought level is higher than the nominal while the far range nodes still shows a low signal.

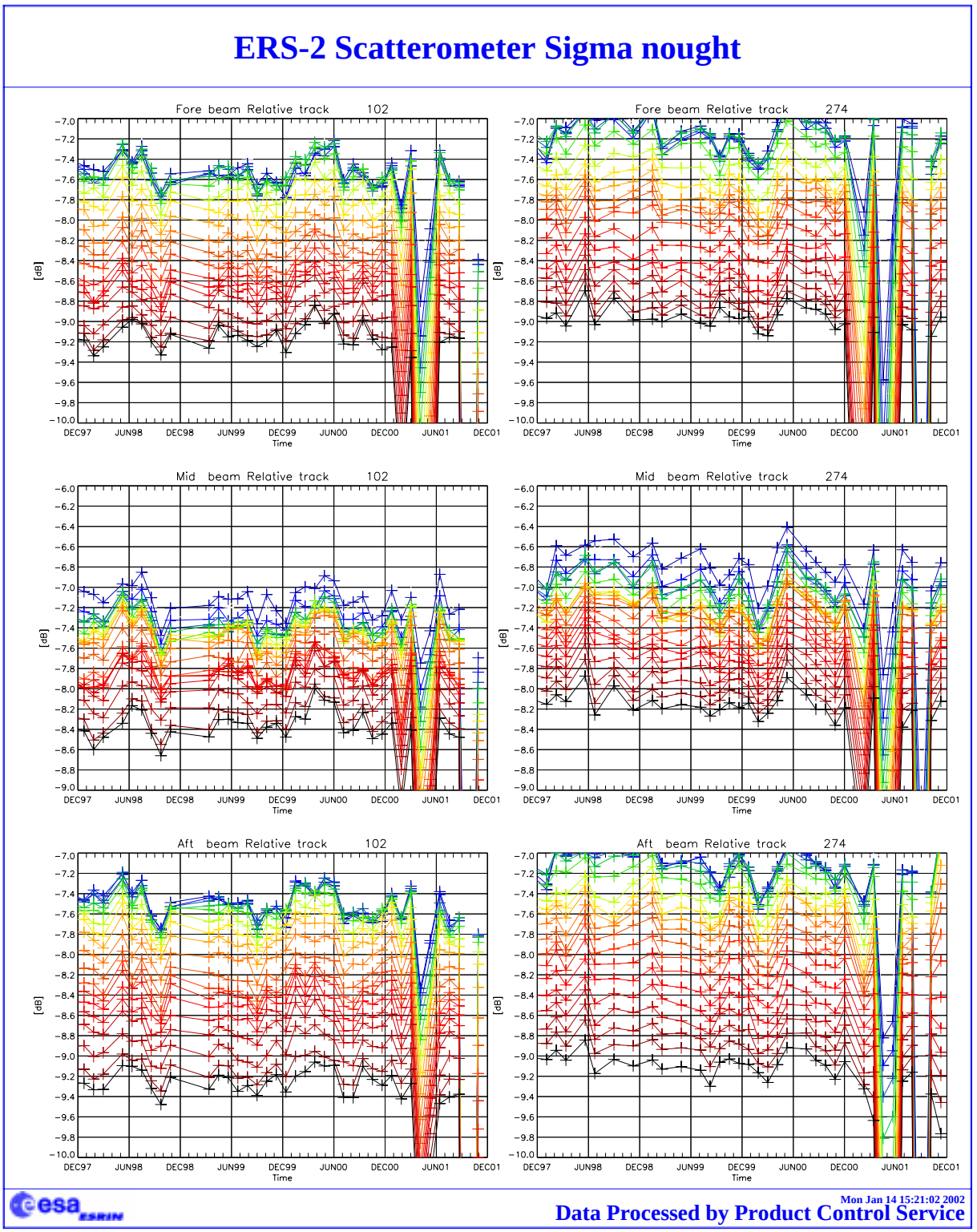

FIGURE 16. Sigma nought over the test area: ascending passes relative tracks 102 (left panels) and 274 (right panels); all nodes across the swath (since December 1997).

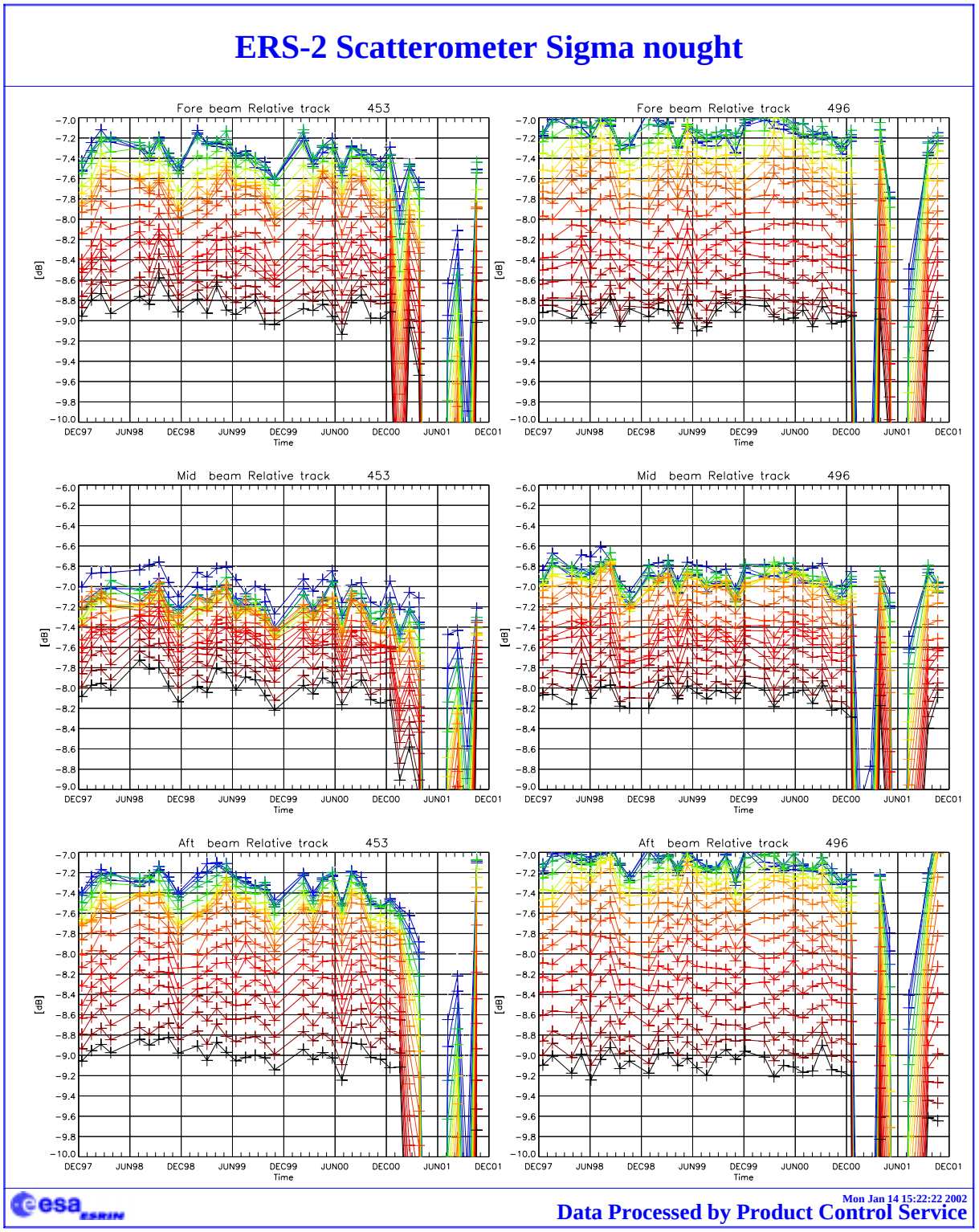

FIGURE 17. Sigma nought over the test area: descending passes relative tracks 453 (left panels) and 496 (right panels); all nodes across the swath (since December 1997).

2.3.6 Antenna temperature evolution over the Rain Forest

The monitoring of the antenna temperature over the Brazilian rain forest is performed by PCS. The antenna temperatures are retrieved from the satellite telemetry when the Scatterometer swath is over the test site and the instrument is active (AMI in wind only or wind/wave mode). The scope of this monitoring is to investigate a possible correlation between the antenna temperatures and the gamma-nought level. This correlation is not clear in the actual data because of the gamma nought variability over the selected area. A deep analysis is to be performed to better understand the facts.

The plots for the three beams and for the ascending, descending and all passes are presented in Figure 18. It is interesting to note that the annual variation is due to the earth inclination and that the antenna temperatures have an increase of roughly 1.0 degree per year in the case of the Mid and Fore antenna and 2 degrees per year for the aft antenna.

This temperature increase could be related to the degradation of the antennae protection film.

An anomalous behaviour of the Fore antenna temperature (only descending passes) has been recorded during the period 7th - 27th June 2001. During that period the temperature was 3 degrees above the nominal level. The temperature increase was related with the instability of the satellite attitude.

The result of the monitoring during the cycle 69 shows that the antenna temperature evolution had a nominal behaviour.

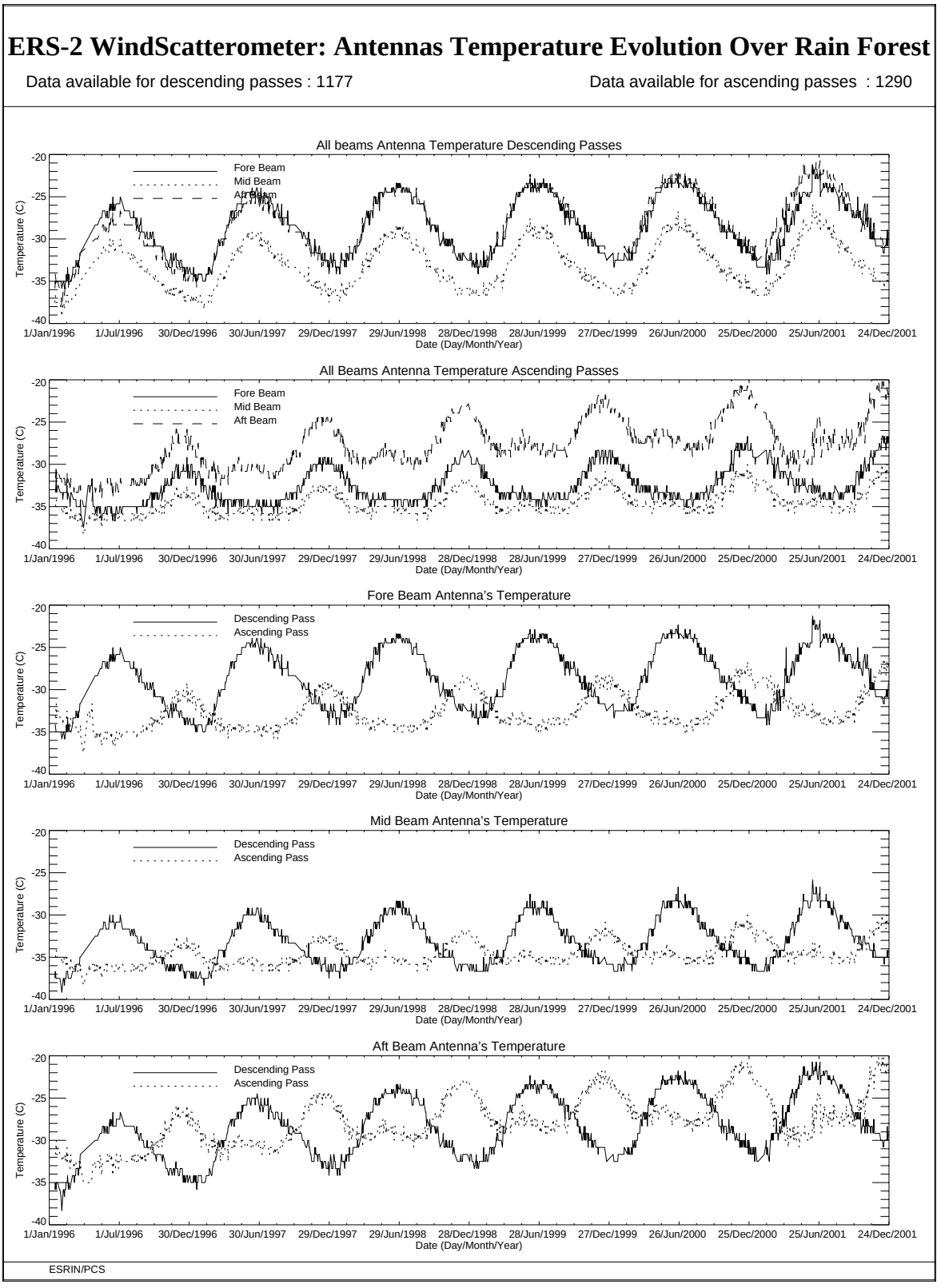

FIGURE 18. ERS-2 Scatterometer: evolution of the antenna temperatures over the Brazilian rain forest.

3.0 Instrument performance

The instrument status is checked by monitoring the following parameters:

- Centre of Gravity (CoG) and standard deviation of the received signal spectrum. This parameter is useful for the monitoring of the orbit stability, the performances of the doppler compensation filter, the behaviour of the yaw steering mode and the performances of the devices in charge for the satellite attitude (e.g. gyroscopes, Earth sensor, Sun sensor).
- Noise power I and Q channel.
- Internal calibration pulse power.

the latter is an important parameter to monitor the transmitter and receiver chain, the evolution of pulse generator, the High Power Amplifier (HPA), the Travelling Wave Tube (TWT) and the receiver.

These parameters are extracted daily from the UWI products and averaged. The evolution of each parameter is characterised by a least square line fit. The coefficients of the line fit are printed in each plot.

3.1 Centre of gravity and standard deviation of received power spectrum

The Figure 19 shows the evolution of the two parameters for each beam.

The tendency from the beginning of the mission to the operation with the new Attitude On-board Control System (AOCS) configuration (7th February 2000) is a clear and regular increase of the Centre of gravity (CoG) of received spectrum for the three antennae. An increase of roughly 200 Hz was observed at the end of the AOCS qualification period. After the AOCS commissioning phase this parameter further evolved.

The old AOCS configuration (one Digital Earth Sensor - DES, one Digital Sun Sensor - DSS and 3 gyros) is no more considered safe because 3 of the six gyros on-board are out of order or very noisy. The new attitude control configuration is designed to pilot the ERS-2 using only one gyro plus the DES and the DSS modules. Scope of this new configuration is to extend the satellite lifetime by using the available gyros one at the time.

For the new AOCS configuration, the gyro 5 was used until 7th October 2000 when it failed. From 10th October 2000 to 24th October 2000 the gyro 6 was used. This explains the decrease of roughly 100Hz in the CoG of the received spectrum. From 25th October 2000 to 17th January 2001 the gyro 1 was used to pilot the ERS-2 satellite.

On 17th January 2001 the AOCS was upgraded. The new configuration allows to pilot the satellite without gyroscopes. Unfortunately a failure of the Digital Earth Sensor (DES A-side) caused ERS-2 to enter in Safe-Mode on the same day. On 25th January 2001 gyro #1 also failed. During the period of safe mode the spacecraft had drifted out of the nominal deadband by some 30 Km. The nominal orbit was reached on 6th February 2001.

In order to preserve the remaining gyroscopes for further manoeuvres, ERS-2 will now being operated in Extra Backup Mode (EBM). The EBM is a coarse attitude control mode. An upgrade of EBM has been performed on 30th March 2001. The aim of the upgrade was to introduce the Yaw steering law inside the piloting function. The new configuration has been renamed as EBM-YSM.

Since 7th June 2001 a new AOCS configuration is active on board. The purpose of the Zero Gyro Mode (ZGM) is to improve the yaw performances without use of gyroscope. The new configuration is under validation by ESOC-ASTRIUM-ESRIN.

Until 17th January 2001 the evolution of the standard deviation of the CoG of the received spectrum was stable apart from the change occurred on 26th, October 1998. On October 26th, 1998 the standard deviation of the CoG had, on average, a decrease of roughly 100 Hz for the fore and aft antenna and of roughly 30Hz for the mid antenna. This change is linked with the increase of the transmitted power (see Section 3.3).

Others changes in the AOCS configuration are recognised in Figure 19. The two steps observed at the beginning of the plots of the CoG (see Figure 19) are due to a change in the pointing subsystem (DES reconfiguration) side B instead of side A after a depointing anomaly (see table 2 for the list of the all AOCS depointing anomaly occurred during the ERS-2 mission). The first change is from 24th, January 1996 to 14th, March 1996, the second one is from 14th February 1997 to 22nd April 1997. During these periods side B was switched on. It is important to note that during the first time a clear difference in the CoG of the received spectrum is present only for the Fore antenna (an increase of roughly 100 Hz) while during the second time the change has affected all the three antennae (roughly an increase of 200 Hz, 50 Hz and 50 Hz for the fore, mid and aft antenna respectively).

Table 2: ERS-2 Scatterometer AOCS depointing anomaly

From	To
24th January 1996 9:10 a.m.	26th January 1996 6:53 p.m
14th February 1997 1:25 a.m.	15th February 1997 3:44 p.m
3rd June 1998 2:43 p.m.	6th June 1998 12:47 a.m.
1st September 1999 8:50 a.m.	2nd September 1999 1:28 a.m.
7th October 2000 4:38 p.m.	10th October 2000 4:49 p.m.
24th October 2000 4:05 p.m.	25th October 2000 12:05 p.m.
17th January 2001	6th February 2001

The Figure 19 shows also when the satellite was operated in Fine Pointing Mode (FPM) in EBM, ZGM mode or the on-board doppler compensation was missing. These events are related with the large peaks in the CoG of the received spectrum plots (fore and aft antenna) and are listed in Table 3.

Table 3: ERS-2 Scatterometer anomalies in the CoG fore and aft antenna

Date	Reason
26th and 27th September 1996	missing on-board doppler coefficient (after cal. DC converter test period)

Date	Reason
6th and 7th June 1998	no Yaw Steering Mode (after depointing anomaly)
2nd and 3rd December 1998	missing on-board doppler coefficients (after AMI anomaly 228)
16th and 17th February 2000	Fine Pointing Mode (FPM) (due to AOCS mono-gyro qualification period)
14th April 2000	Fine Pointing Mode (FPM)
30th May 2000	Fine Pointing Mode (FPM)
5th July 2000	Fine Pointing Mode (FPM) after instrument switch-on
27th September 2000	Fine Pointing Mode (FPM) to up-load AOCS software patch
2nd November 2000	Fine Pointing Mode (FPM)
5th and 6th December 2000	Fine Pointing Mode (FPM) due to orbital manoeuvre
6th February - 30th March 2001	Extra Backup Mode (EBM) coarse attitude control
30th March 2001- 7th June 2001	EBM-YSM gyro-less yaw steering mode
7th June 2001 - onwards	ZGM commissioning phase

The peaks (before February 2001) shown in the plot of mid beam standard deviation of the CoG of the received spectrum are linked to the satellite manoeuvres and AOCS depointing anomaly.

During the cycle 69 a yaw degradation was recorded on days 3rd, 24th November, 12thand 24th December 2001. The cause of that degradation was an increase of the solar activity and the consequent variation of the air-drag. Figure 20 reports the daily average of the CoG of the received spectrum and its standard deviation. **Note that the vertical scale of the plots has been further extended to take into account the period with high solar activity**.

During those days the daily average standard deviation of the CoG of the received spectrum increased up to 6000 Hz for the three scatterometer antenna.

For the daily average of the CoG of the received spectrum the improvement (a CoG closer to 0 hz) noted since 8th November vanished around 28th November 2001.

In Figure 21 is plotted, with different colours, the three days averaged CoG of the received spectrum (mid antenna) as time function from the ascending node (time = 0). Each unit of the X axis is 5 seconds from the ascending node while the Y axis is the frequency in Hz. The curves are obtained by filtering the evolution of the CoG of the received spectrum throughout the orbit. **Note that the vertical scale in Figure 21 has been extend from +/- 1.5 Khz to +/- 4.0 Khz to take into account the increase of the fluctuation.**

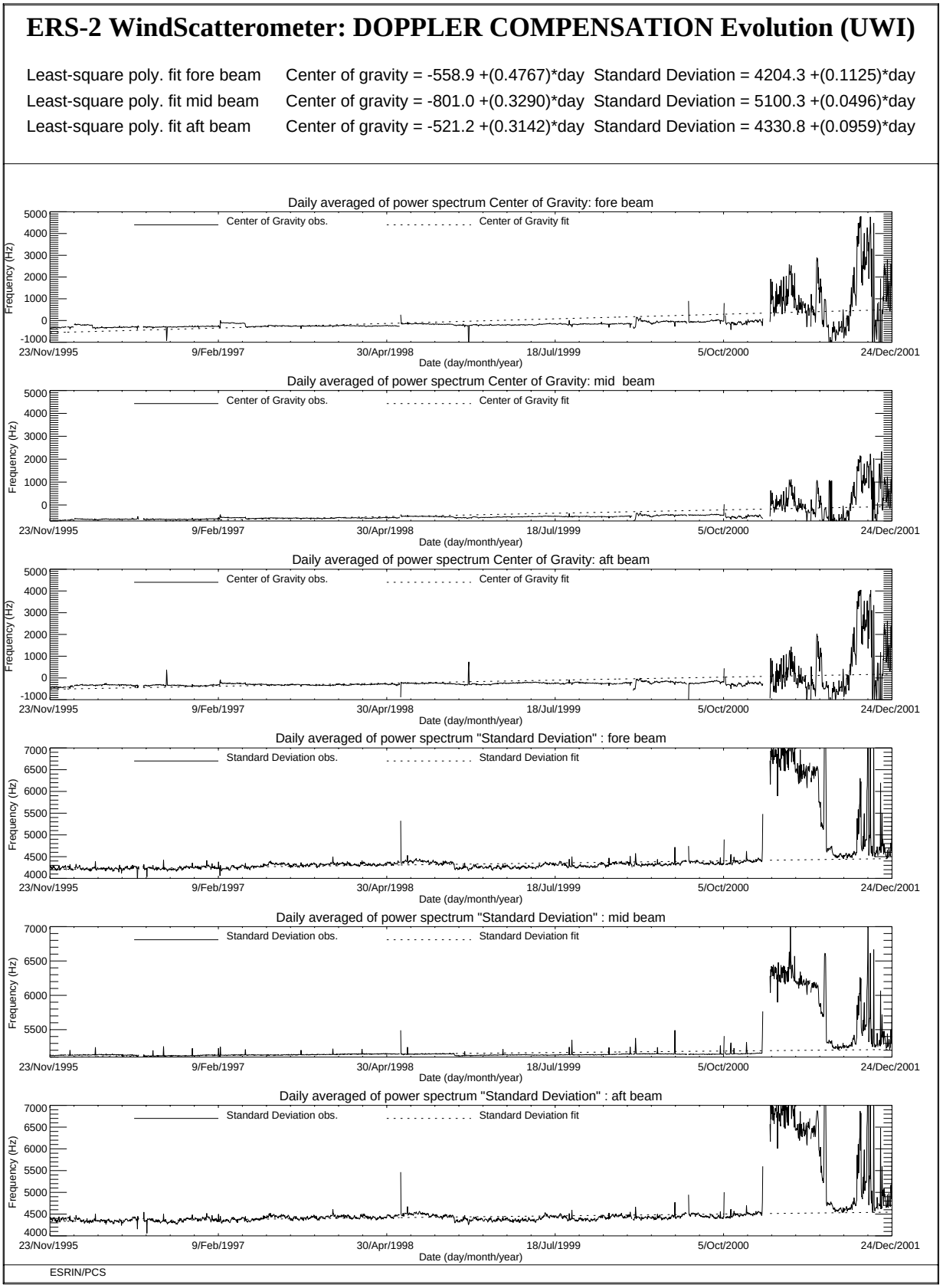

FIGURE 19. ERS-2 Scatterometer: Centre of Gravity and standard deviation of received power spectrum since the beginning of the mission.

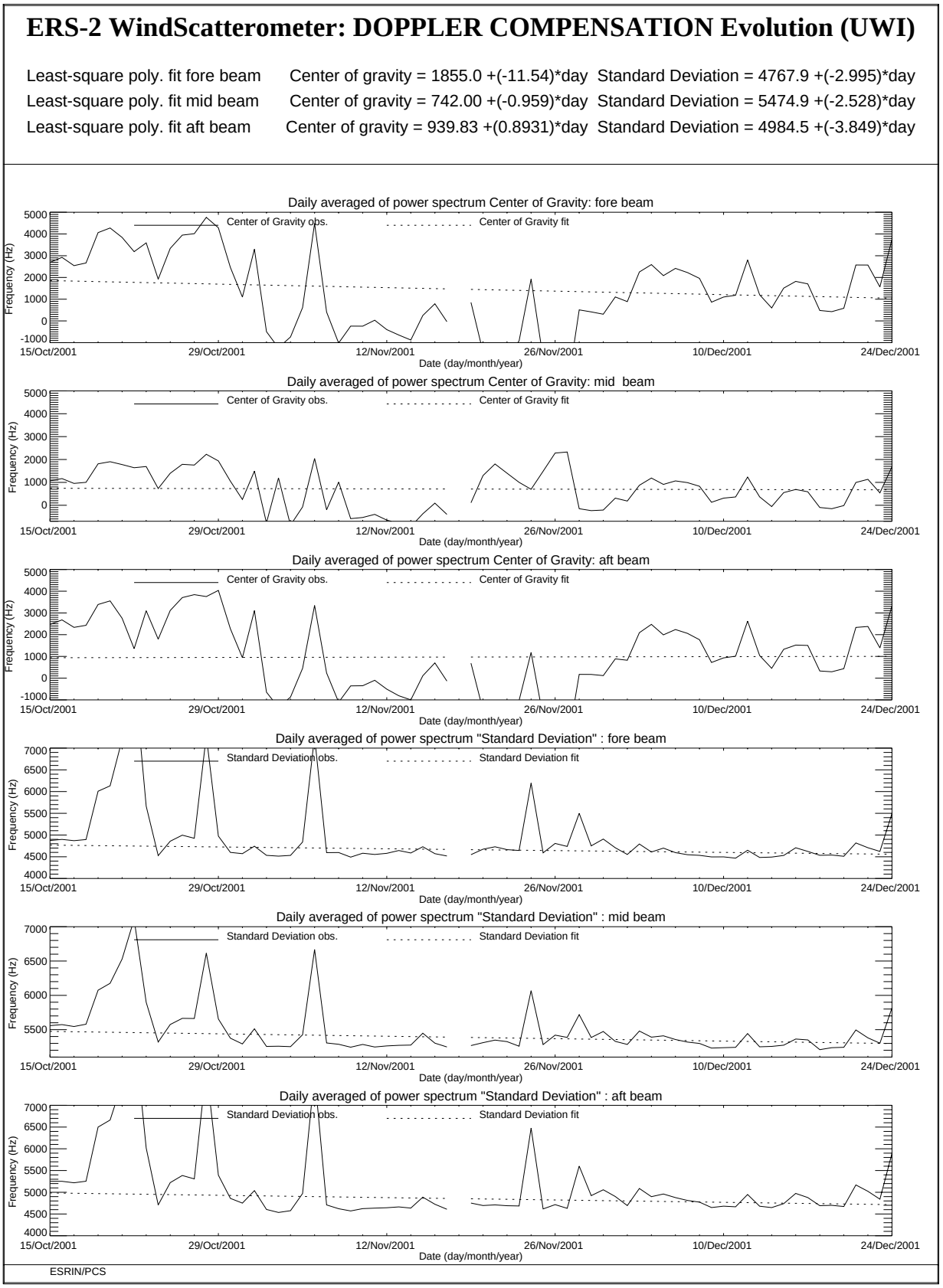

FIGURE 20. ERS-2 Scatterometer: Centre of Gravity and standard deviation of received power spectrum during the cycle 69.

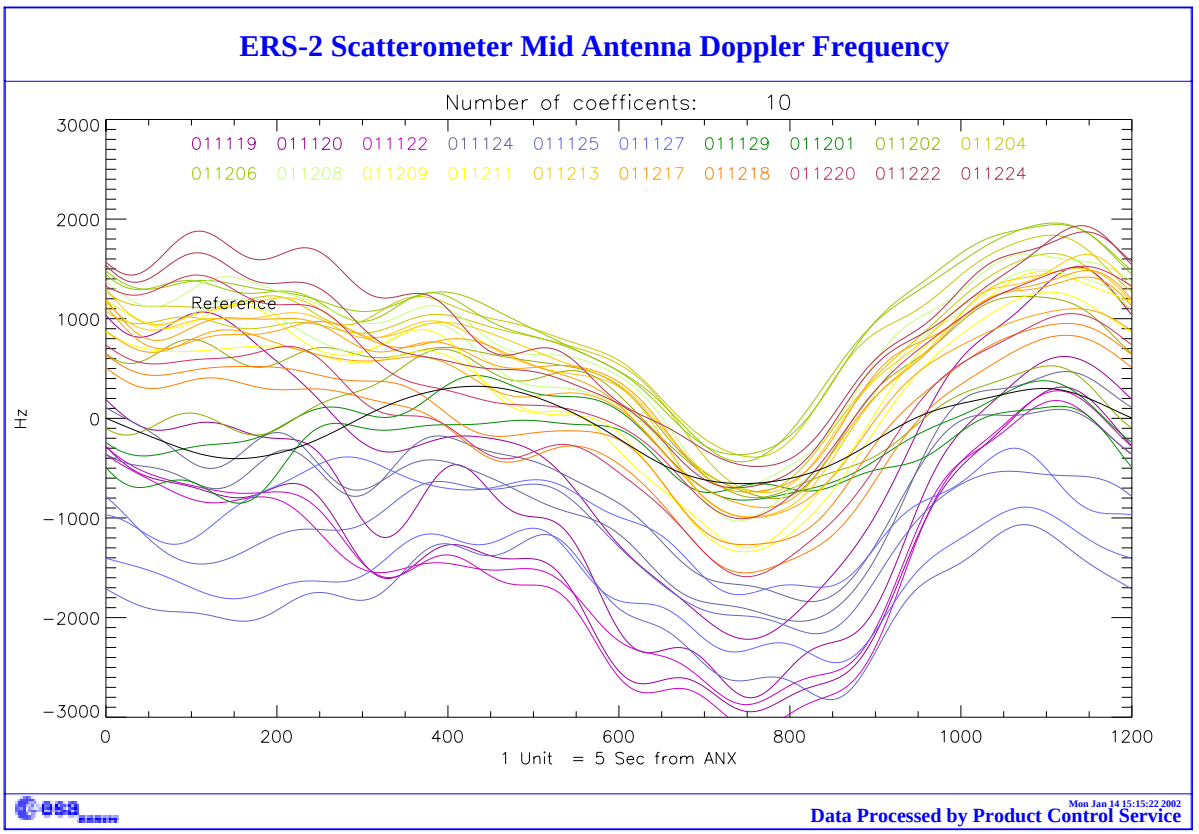

FIGURE 21. Low pass filtered evolution of the Mid beam CoG as function of ascending node time (1 unit 5 s.) cycle 69.

3.2 Noise power level I and Q channel

The results of the monitoring are shown in Figure 22. The first set of three plots presents the noise power evolution for the I channel while the second set shows the Q channel. The noise level is less than 1 ADC Unit for the fore and aft signals and is negligible for the mid one. From the plots one can see that the noise level is more stable in the I channel than in the Q one. The PCS suspects that an explanation should be found in the different position of the receivers, in particular it seems that the Q one is closer to the ATSR-GOME electronics. A confirmation of this hypothesis has been asked to ESTEC.

Since 5th December 1997 some high peaks appear in the plots. These high values for the daily mean are due to the presence for these special days of a single UWI product with an unrealistic value in the noise power field of its Specific Product Header. The analysis of the raw data used to generate these products lead in all cases to the presence of one source packet with a corrupted value in the noise field stored into the source packet Secondary Header. Table 4 presents the list of the UWI products affected by a corrupted noise field and disseminated during cycle 69.

Table 4: UWI products with noise field corrupted (cycle 69)

Noise Field corrupted	Noise value (ADC Unit)	Acquisition Time
None	-	-

The reason why noise field corruption is beginning from 5th December 1997 is at present unknown. It is interesting to note that at the beginning of December 1997, we started to get as well the corruption of the Satellite Binary Times (SBTs) stored in the EWIC product. The impact in the fast delivery products was the production of blank products starting from the corrupted EWIC until the end of the scheduled stop time. A change in the ground station processing in March 1998 overcame this problem.

Since 9th August 1998 some periods with a clear instability in the noise power have been recognised. Table 5 gives the detailed list.

Table 5: ERS-2 Scatterometer instability in the noise power

From	To
9th August 1998	26th October 1998
29th November 1998	6th December 1998
23rd December 1998	24th December 1998
7th June 1999	10th June 1999
17th August 1999	22nd August 1999
8th September 1999	9th September 1999
3rd October 1999	8th October 1999
16th October 1999	18th October 1999
26th October 1999	28th October 1999

From	To
25th December 1999	2nd January 2000
10th February 2000	11th February 2000
19th March 2000	26th March 2000

To better understand the instability of the noise power the PCS has carried out investigations in the scatterometer raw data (EWIC) to compute the noise power with more resolution. The result is that for the orbits affected by the instability the noise power had a decrease of roughly 0.7 dB for the fore and aft signals and a decrease of roughly 0.6 dB in the mid beam case (see the report for the cycle 42).

The decrease of the noise power during the orbits affected by the instability is comparable with the decrease of the internal calibration level that occurred during the same orbits. The reason of this instability (linked to the AMI anomalies) is still under investigation. A plot that shows the correlation among the noise power, the internal calibration level and the AMI anomaly is reported in section 3.3.

Figure 23 shows the evolution of the noise power since 26th October when 2 dB were added to the transmitted power. The periods with the instability in the noise power are clear shown in the plots in particular for the fore and aft beam signals.

The noise power decrease noted on 6th June 2001 is related with continuous wave operation around the orbit. The reduction of the noise is an artifact due to on-board data processing. In fact all noise samples taken during 32 FMA sequence are squared and averaged over 896 samples. In wind-wave mode 2 FMA sequences are missing (to acquire SAR imagette) but the average is still computed over 896 samples (see ER-SS-MSS-AM-0700 sheet 167).

During cycle 69 the monitoring of the noise power shows a stable result.

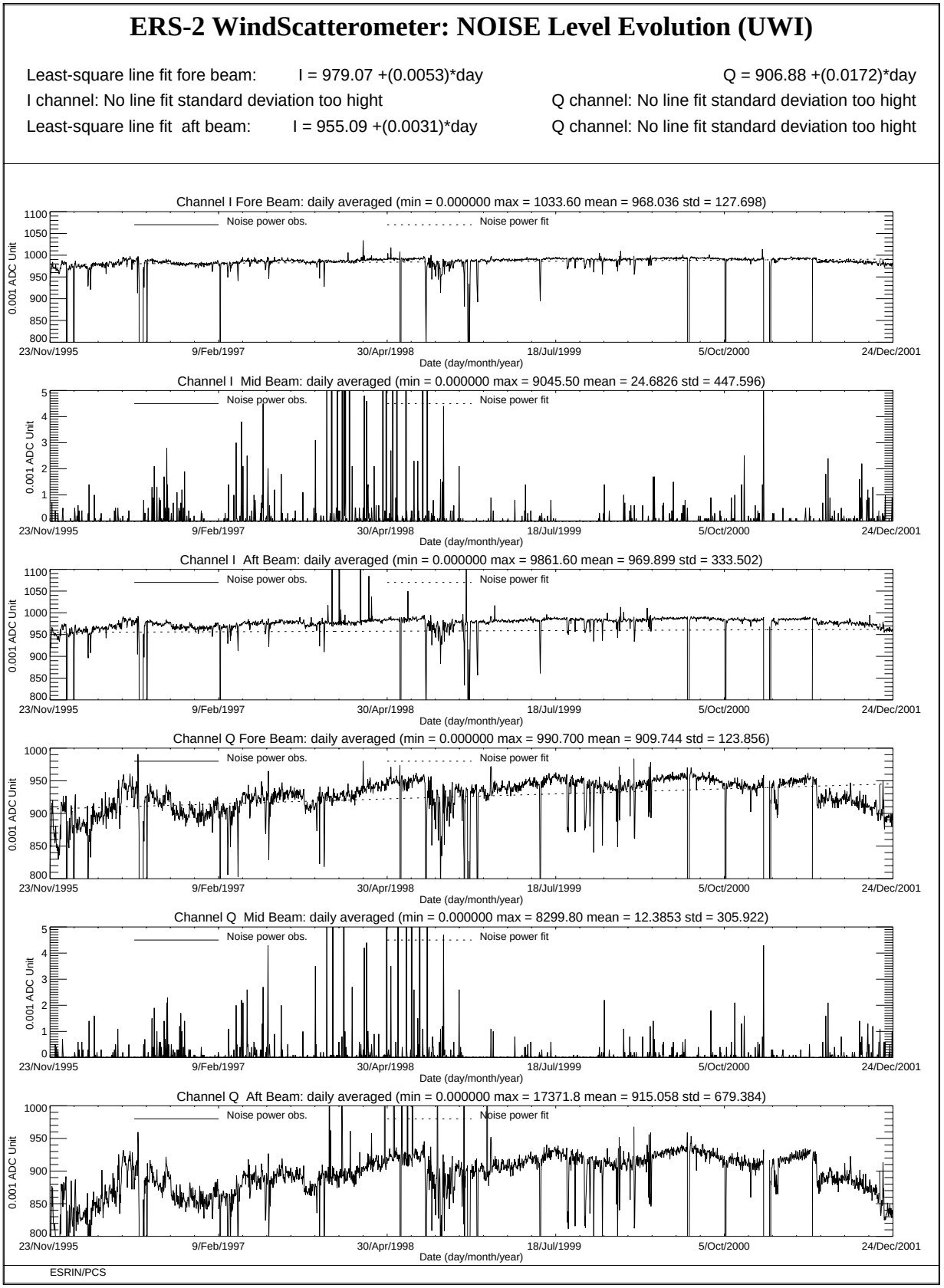

FIGURE 22. ERS-2 Scatterometer: noise power I and Q channel since the beginning of the mission.

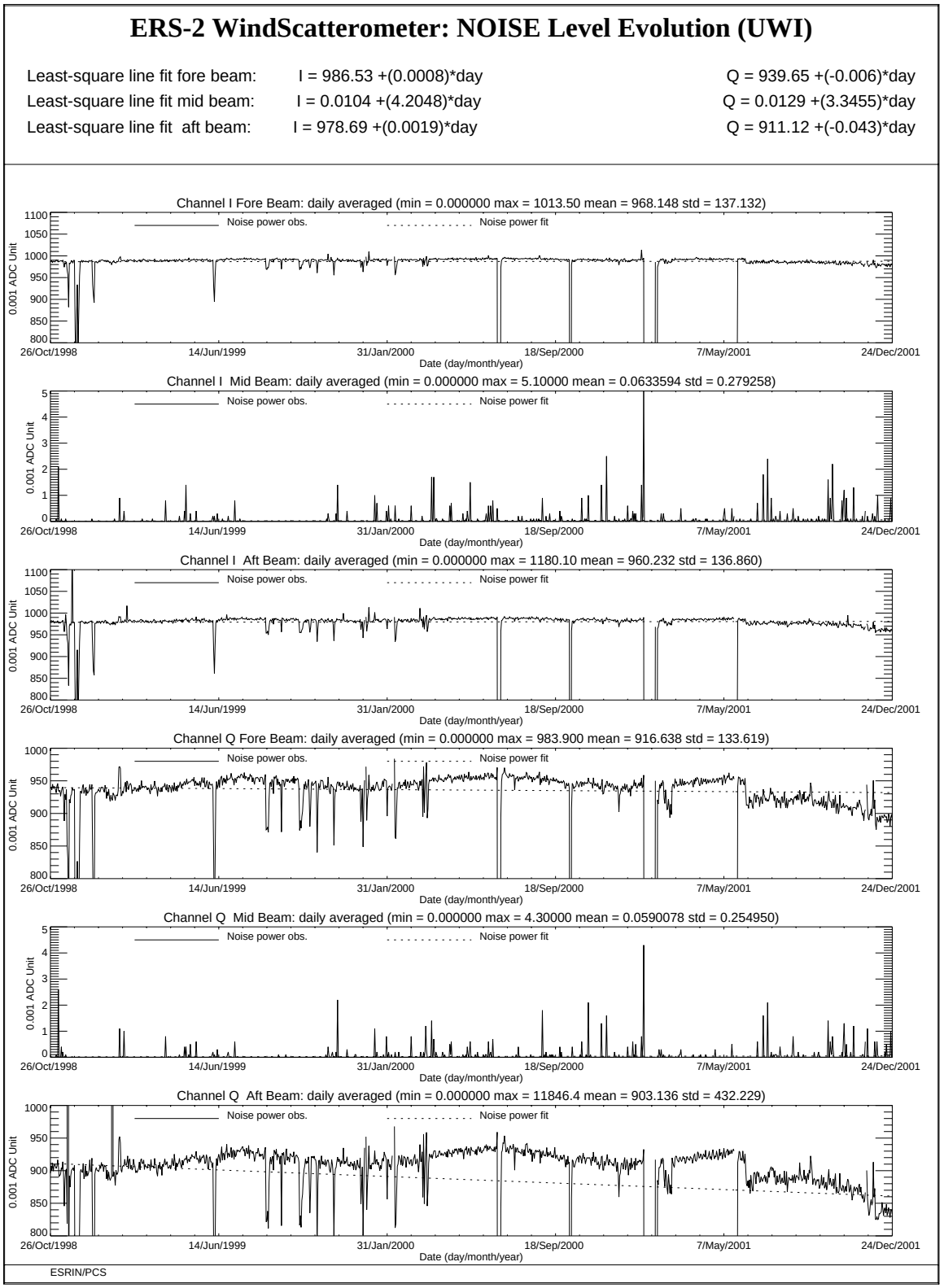

FIGURE 23. ERS-2 Scatterometer: noise power I and Q channel since 26th October 1998 when the transmitted power was increased by 2 dB.

3.3 Power level of internal calibration pulse

For the internal calibration level, the results, since the beginning of the mission, are shown in Figure 25.

The high value of the variance in the fore beam until August, 12th 1996 is due to the ground processing. In fact all the blank source packets ingested by the processor were recognized as Fore beam source packets with a default value for the internal calibration level. The default value was applicable for ERS-1 and therefore was not appropriate for ERS-2 data processing. On August 12th, 1996 a change in the ground processing LUT overcame the problem.

Since the beginning of the mission a power decrease is detected. The power decrease is regular and affects the AMI when it is working in wind-only mode, wind/wave mode and image mode indifferently.

The reason is that the TWT is not working in saturation, so that a variation in the input signal is visible in the output. The variability of the input signal can be two-fold: the evolution of the pulse generator or the tendency of the switches between the pulse generator and the TWT to reset themselves into a nominal position. These switches were set into an intermediate position in order to put into operation the scatterometer instrument (on 16th November 1995).

After the change of the calibration subsystem on August 6th, 1996 the decrease is more evident and it is estimated in 0.09 dB per cycle (0.0025 dB/day).

On 26th October 1998 (cycle 37) to compensate for this decrease, 2.0 dB were added to the Scatterometer transmitted power and this explains the large step shows in Figure 25 and Figure 24. After that day the power decrease is on average 0.08 dB per cycle (0.0022 dB/day).

It is important to point out the efficiency of the internal calibration for keeping the absolute calibration level stable. In fact, no important change is noted in the monitoring of the gamma-nought level over the Brazilian rain forest during the power decrease and after the increase of the transmitted power (see section 2.0).

Since 9th August 1998 the internal calibration level shows an instability. This instability is very well correlated with the fluctuations observed in the noise power as outlined in section 3.2.

Figure 24 shows the daily average of the internal calibration and the noise power from 1st August 1998 to 6th August 2001. In the figure are also reported the anomalies that affected the AMI and the platform (the triangles in the plot) and the days when the instability was very strong (asterisks in the plot).

From Figure 24 it seems that there is a clear correlation between the instability (noise and calibration level) and the AMI anomalies.

On 13th July 2000 an high peak (+3.5 dB) was detected in the transmitted power. This event has been investigated deeply by PCS and ESOC. The results of the analysis are reported in the technical note “ERS-2 Scatterometer: high peak in the calibration level” available in the PCS. The high transmitted power was obtained after an arc event which occurred inside the HPA. After that event the calibration level had an average increase of roughly 0.14 dB.

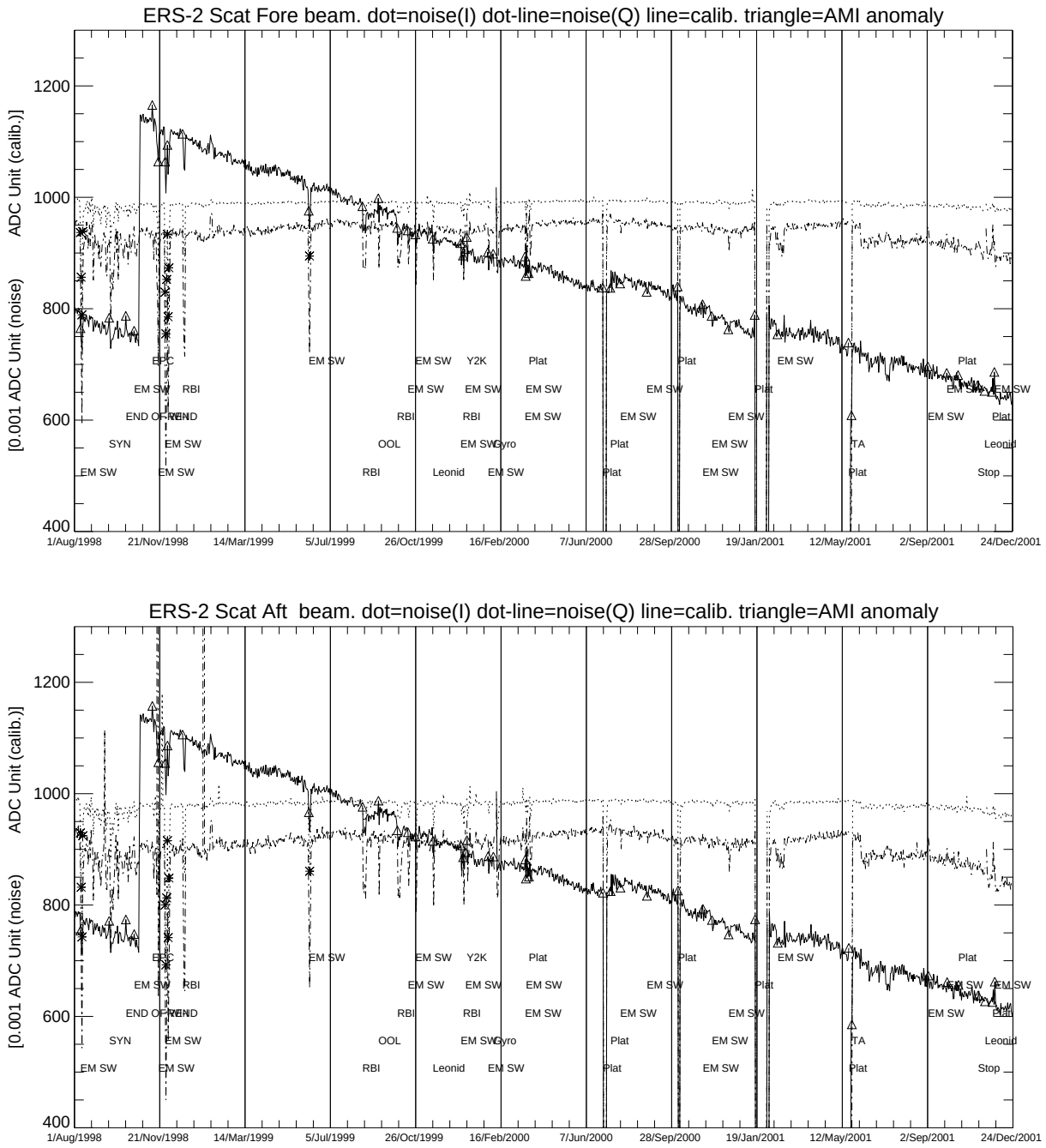

FIGURE 24. ERS-2 Scatterometer: noise power (I and Q channel) and internal calibration power evolution from 1st August 1998 to 19th March 2001. Upper panel Fore antenna, lower panel Aft antenna.

During the cycle 69, on average, the power decrease was 0.15 dB/Cycle. The actual level is roughly 0.83 dB below the level reached on October 1998.

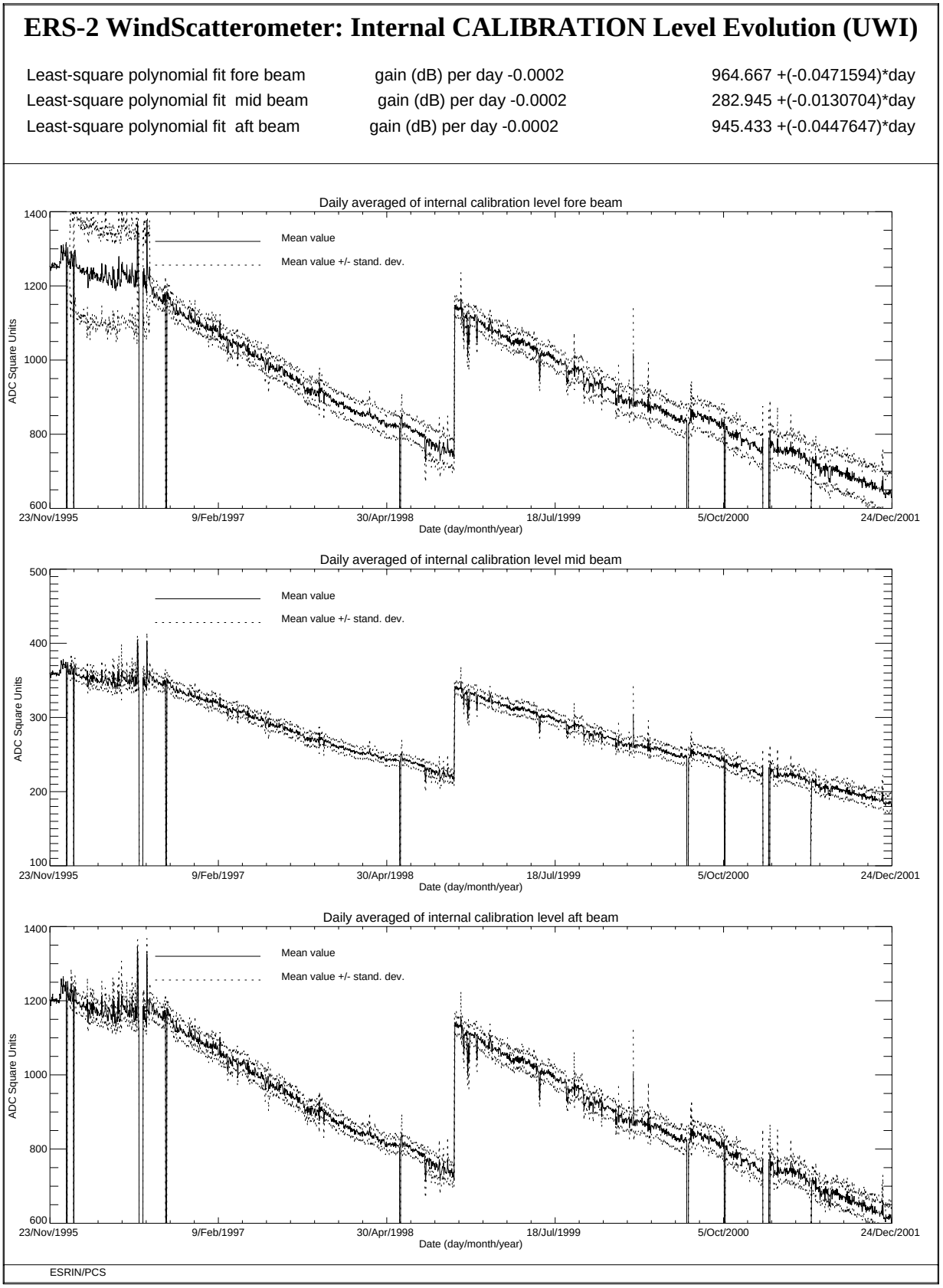

FIGURE 25. ERS-2 Scatterometer: power of internal calibration pulse since the beginning of the mission.

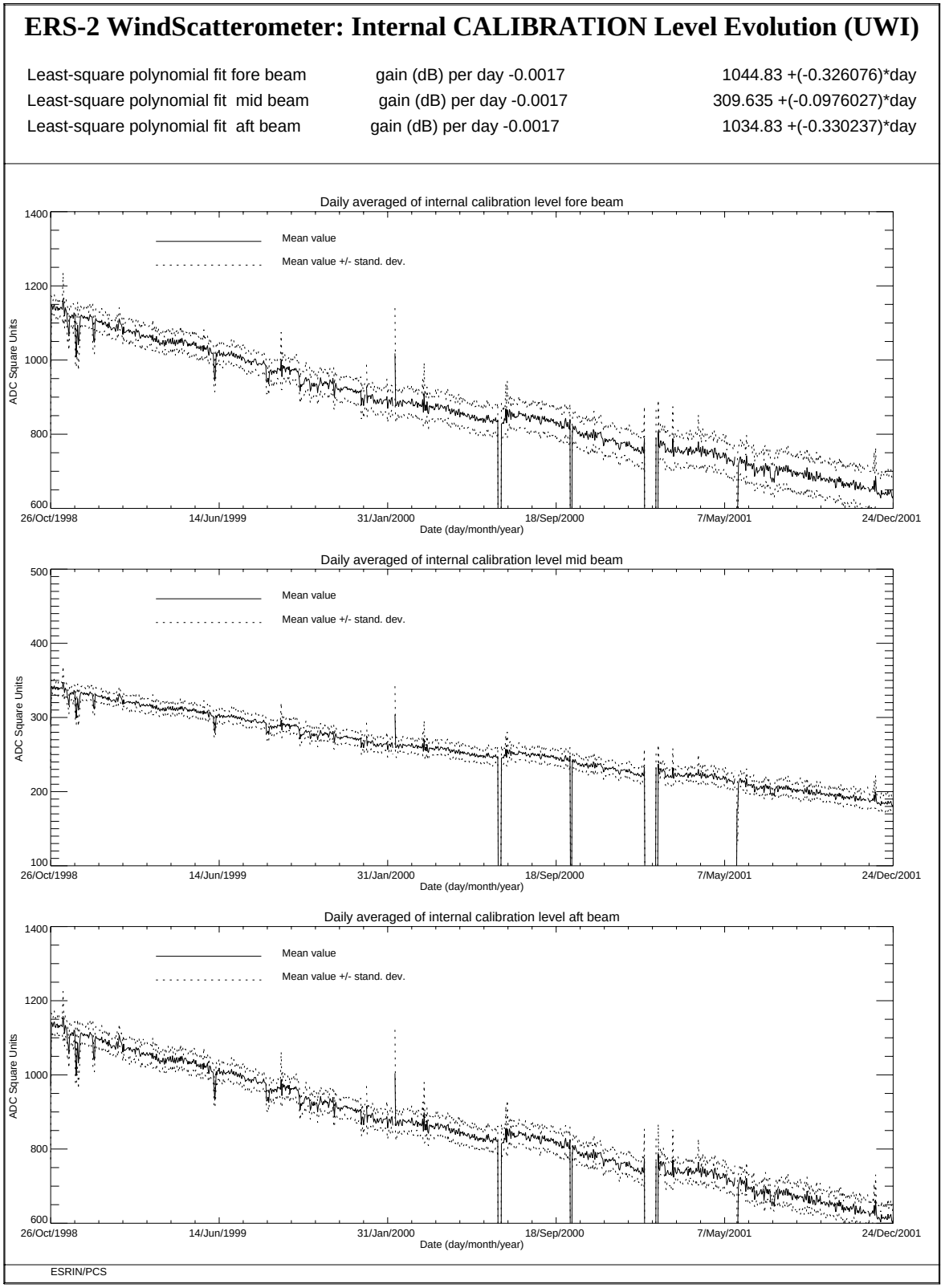

FIGURE 26. ERS-2 Scatterometer: power of internal calibration level since 26th October 1998 when the transmitted power was increased by 2.0 dB.

4.0 Products performance

One of the most important point in the monitoring of the products performance is their availability. The Scatterometer is a part of ERS payload and it is combined with a Synthetic Aperture Radar (SAR) into a single Active Microwave Instrument (AMI). The SAR users requirements and the constraints imposed by the on-board hardware (e.g. amount of data that can be recorded in the on-board tape) set rules in the mission operation plan.

The principal rules that affected the Scatterometer instruments are:

- over the Ocean the AMI is in wind/wave mode (scatterometer with small SAR imagettes acquired every 30 sec.) and the ATSR-2 is in low rate data mode.
- over the Land the AMI is in wind only mode (only scatterometer) and the ATSR-2 is in high rate mode. (Due to on board recorder capacity, ATSR-2 in high rate is not compatible with Sar wave imagette acquisitions.)

This strategy preserves the Ocean mission.

Moreover:

- the SAR images are planned as consequence of users' request.

These rules have an impact on the Scatterometer data availability.

Figure 27 shows the AMI operational modes. Each segment of the orbit has different colour depending on the instrument mode: brown for wind only mode, blue for wind-wave mode and green for image mode. The red and yellow colours correspond to gap modes (no data acquired).

Due to ZGM commissioning phase the AMI was operated in wind-wave mode throughout the orbits. For that reason the "nominal" data gaps between Australia and Antarctic and between Africa and Antarctic are vanished (see the previous Wind Scatterometer cyclic reports). Those data gaps were due to AMI switches from wind/wave to wind only mode.

For cycle 69 the percentage of the ERS-2 AMI activity is shown in table 6.

Table 6: ERS-2 AMI activity (cycle 69)

AMI modes	ascending passes	descending passes
Wind and Wind-Wave	**91.0%**	**88.1%**
Image	**1.4%**	**5.4%**
Gap and others	**8.6%**	**6.5%**

Table 7 reports the major data lost due to the test periods and AMI or satellite anomalies occurred after August 6th, 1996 (before that day for many times data were not acquired due to the DC converter failure).

Table 7: ERS-2 Scatterometer mission major data lost after 6th, August 1996

Start date	Stop date	Reason
September 23rd, 1996	September 26th, 1996	ERS-2 switched off due to a test period
February 14th, 1997	February 15th, 1997	ERS-2 switched off due to a depointing anomaly
June 3rd, 1998	June 6th, 1998	ERS-2 switched off due to a depointing anomaly
November 17th, 1998	November 18th, 1998	ERS-2 switched off to face out Leonide meteo storm
September 22nd 1999	September 23rd 1999	ERS-2 switched off due to Year 2000 certification test
November 17th, 1999	November 18th, 1999	ERS-2 switched off to face out Leonide meteo storm
December 31st,1999	January 2nd, 2000	ERS-2 switched off Y2K transition operation
February 7th,2000	February 9th, 2000	ERS-2 switched off due to new AOCS s/w up-link
June 30th, 2000	July 5th, 2000	ERS-2 Payload switched-off after RA anomaly
July 10th, 2000	July 11th, 2000	ERS-2 Payload reconfiguration
October 7th, 2000	October 10th, 2000	ERS-2 Payload switched-off after AOCS anomaly
January 17th, 2001	February 5th, 2001	ERS-2 Payload switched-off due to AOCS anomaly
May 22nd, 2001	May 24th, 2001	ERS-2 Payload switched-off due to platform anomaly
May 25th, 2001	May 25th, 2001	AMI switched-off due thermal analysis
November 17th, 2001	November 18th, 2001	ERS-2 switched off to face out Leonide meteo storm
November 27th, 2001	November 28th, 2001	ERS-2 payload off due to 1Gyro Coarse Mode commissioning

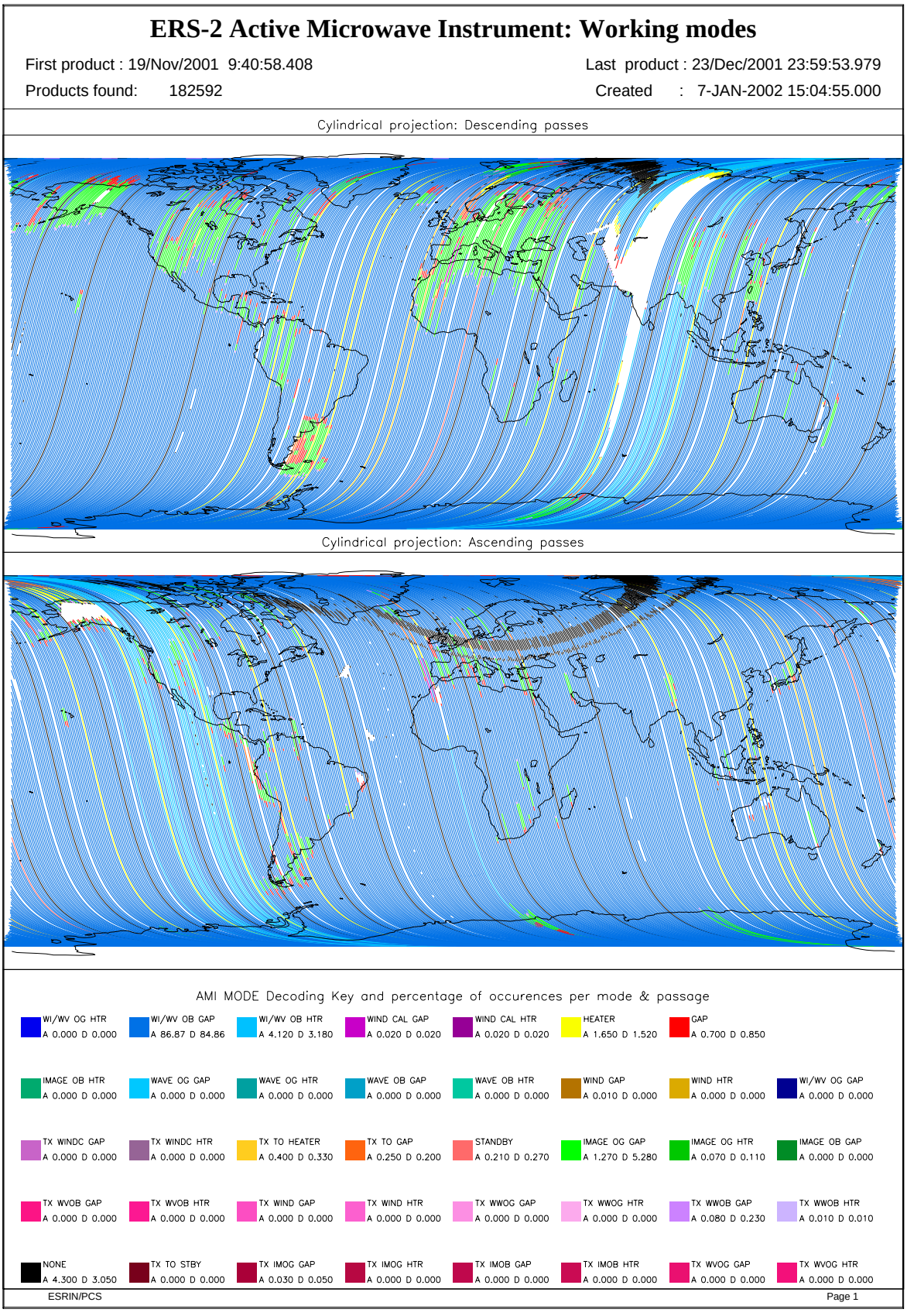

FIGURE 27. ERS-2 AMI activity during cycle 69.

The PCS carries out a quality control of the winds generated from the WSCATT data. The activity is split in two main areas: the first one includes a routine analysis of the fast Delivery Products disseminated to the users, the second one is focused on the improvement of the CMOD-4 (the operative ESA wind retrieval algorithm) for high wind speed (for more information see on the Web site http://pcswww.esrin.esa.it the Cyclone Tracking home page). External contributions to this quality control come also from ECMWF and UK-Met Office.

The routine analysis is summarized in the plots of figure 28; from top to bottom:

- the monitoring of the valid sigma-nought triplets per day.
- the evolution of the wind direction quality. The ERS wind direction (for all nodes and only for those nodes where the ambiguity removal has worked properly) is compared with the ECMWF forecast. The plot shows the percentage of nodes for which the difference falls in the range -90.0, +90.0 degrees.
- the monitoring of the percentage of nodes whose ambiguity removal works successfully.
- the comparison of the wind speed deviation: (bias and standard deviation) with the ECMWF forecast.

The results since August 6th, 1996 until EBM operations can be summarized (apart from the events given in Table 7) as:

- a stable number of valid sigma-nought acquired per day with a small increase after June 29th, 1999 due to the dissemination in fast delivery of the data acquired in the Prince Albert station.
- an accurate wind direction for roughly 93% of the nodes, a success in the ambiguity removal for more than 90.0% of the nodes.

The ERS-2 wind speed shows an absolute bias of roughly 0.5 m/s and a standard deviation that ranges from 2.5 m/s to 3.5 m/s with respect to the ECMWF forecast. The wind speed bias and its standard deviation have a seasonal pattern due to the different winds distribution between the winter and summer season.

It is important to note that only after the end of calibration phase (mid March 1996) the wind products have reached high quality.

Two important changes affect the speed bias plot: the first is on June 3rd, 1996 and it is due to the switch from ERS-1 to ERS-2 data assimilation in the meteorological model. The second change, which occurred at the beginning of September 1997, is due to the new monitoring and assimilation scheme in ECMWF algorithms (4D-Var).

Since 19th April 1999 two set of meteo-table (meteorological forecast centred at 00:00 and 12:00 of each day) are used in the ground processing. With this new strategy the data are processed using the 18 and 24 hours meteorological forecast instead of the 18, 24, 30 36 hours forecast. The data processed with the 18-24 hours tables instead of 30-36 hours tables have an increase in the number of ambiguity removed nodes but no important improvements are shown, on average, in the daily statistics.

Since 25th August 1999 a new LRDPF software (version 8500) is operative in the ground stations. With this upgrade the LRDPF is year 2000 compatible; no changes were introduced in the scatterometer data processing.

The mono-gyro AOCS configuration (see report for cycle 50) that was operative from 7th February 2000 to 17th January 2001 did not affect the wind data performance.

The new AOCS configuration (gyro-less EBM) had a very negative impact in the data quality.

The number of valid nodes has a clear drop from 190000 per day to 9000 per day. The overall Scatterometer transfer function is not matched with the received echo (Doppler shift in the received signal due to degraded satellite attitude) and this fact caused the decrease of the signal to noise ratio and as consequence many nodes are discarded by the wind retrieval algorithm. Moreover the sigma nought are not calibrated (the distance to the cone is high, in particular for the nodes at far range) and the wind speed bias is around 1.5 m/s.

During the ZGM commissioning phase an improvements in the number of valid nodes has been noted. The improvement is mainly linked with the increase of the signal to noise ratio.The number of valid nodes passed from 9000 per day (EBM) to 16000 per day during the ZGM commissioning (end of July 2001).

During the cycle 69 the wind speed bias stayed stable around 0.3 m/s. The wind speed standard deviation was around 3 m/s.

Since 17th January 2001 no Scatterometer data were disseminated to the users.The reason is because the actual ground processing is not able to assure calibrated data and the quality of the wind products is very poor. To overcome the problem, a re-design of the ground processor is ongoing.

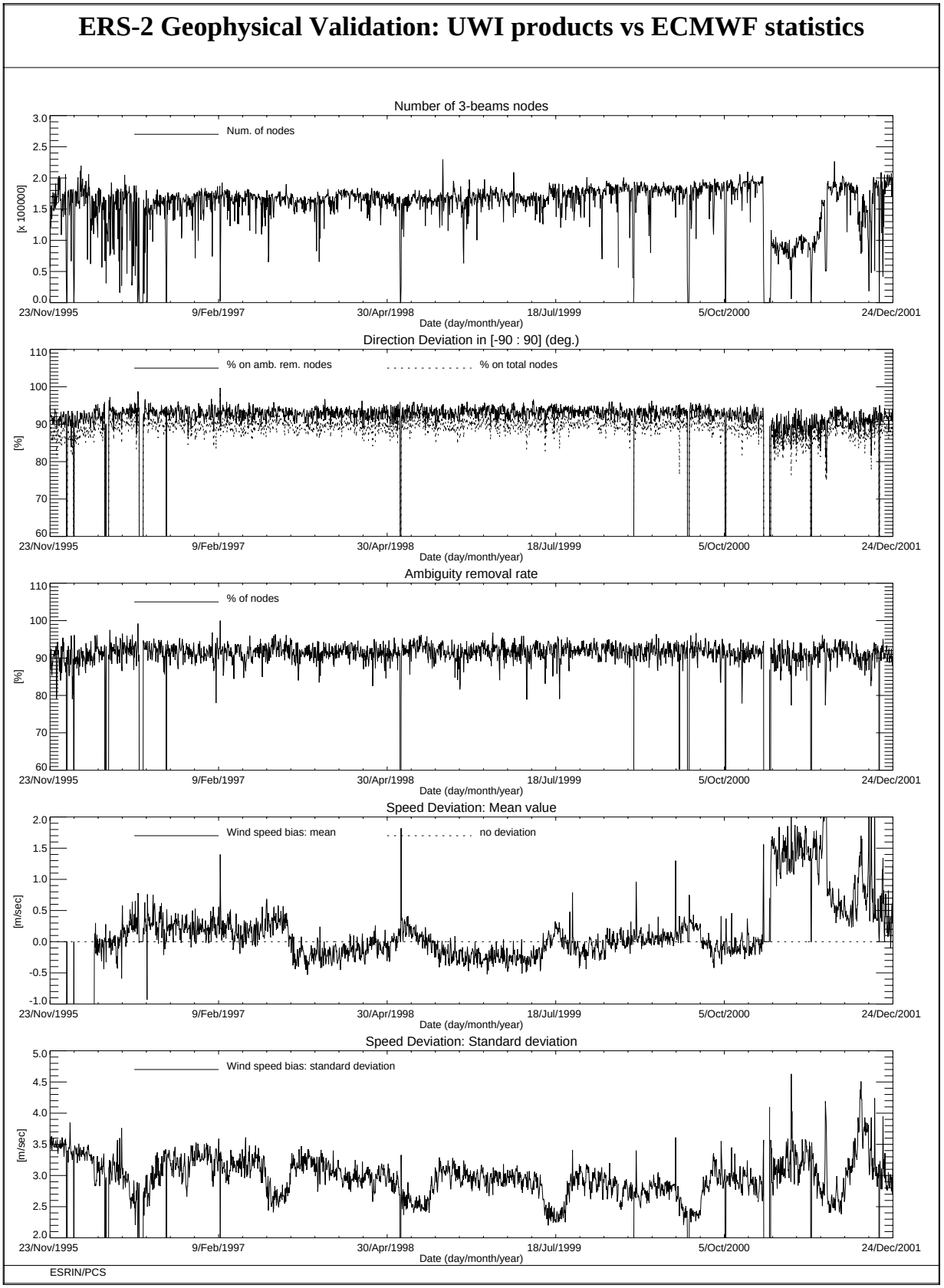

FIGURE 28. ERS-2 Scatterometer: wind products performance since the beginning of the mission.

5.0 Yaw error angle estimation

This section reports the results regarding the estimation of the yaw error angle. That estimation was done by analysing the Scatterometer raw data. Thanks to the satellite data link DDS, raw data dumped in Kiruna station are transferred in ESRIN with a delay of few hours. The PCS at ESRIN had developed a prototype for a coarse estimation of the yaw error angle. Details regarding the algorithm used are available in the Technical note " Impact of a yaw error angle in the Scatterometer Doppler Frequency".

The study carried out in ESRIN shows that the main problem in the yaw estimation is the received signal bandwidth that is limited by the on-board low pass filter. As consequence only small yaw angle (within +/- 3 deg) can be estimated.

The prototype developed in ESRIN has been tested against the SAR wave yaw angle estimator also developed in ESRIN. As expected there is a good agreement between the two estimation in particular for small error angles. The Figure 29 shows a result of the validation for orbits 33907 and 33921.The bold line is the yaw error angle estimated from Scatt data while the thin line is the estimation done by SAR wave data.

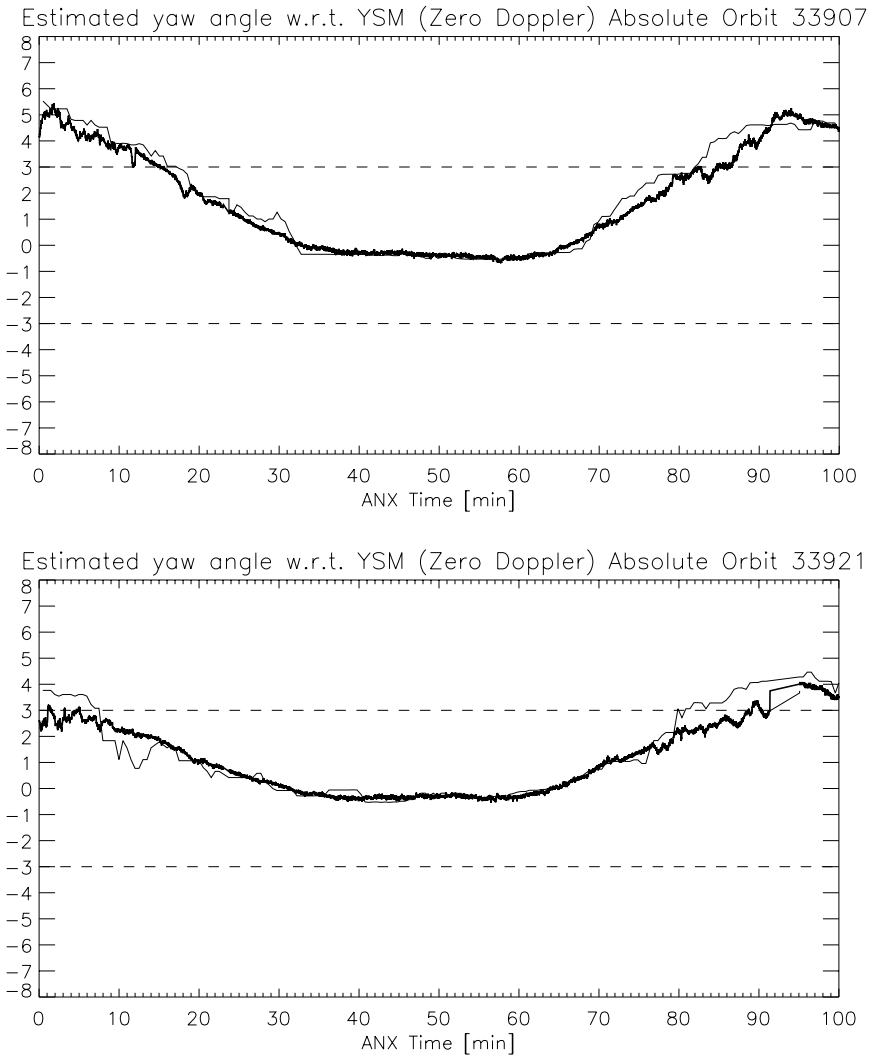

FIGURE 29. Yaw evolution along orbit 33907 (upper panel) and 33921 (down panel)

The Figure 30 shows the evolution of the averaged (per orbit) yaw error angle since the beginning of the ZGM commissioning (June 2001). The orbit processed are only the ones dumped at Kiruna station (roughly 66% of the total). Missing orbits are indicated with a black dot. The Figure 30 shows only the orbits that had passed a quality control. Orbits with a yaw standard deviation greater than 1 deg. and with an absolute bias above 3 deg. had been flagged as bad quality (red dot in the plot). It is foreseen that for those orbit will not be possible to retrieve calibrated sigma noughts. From June 2001 the bad quality orbits are roughly 60%. That result is mainly due to the tuning of the AOCS parameters in June 2001 and strong solar activity in October and November 2001.

The Figure 31 shows the same of Figure 30 for the cycle 69. As reported in the plot the orbits with bad quality are only 25% of the total.

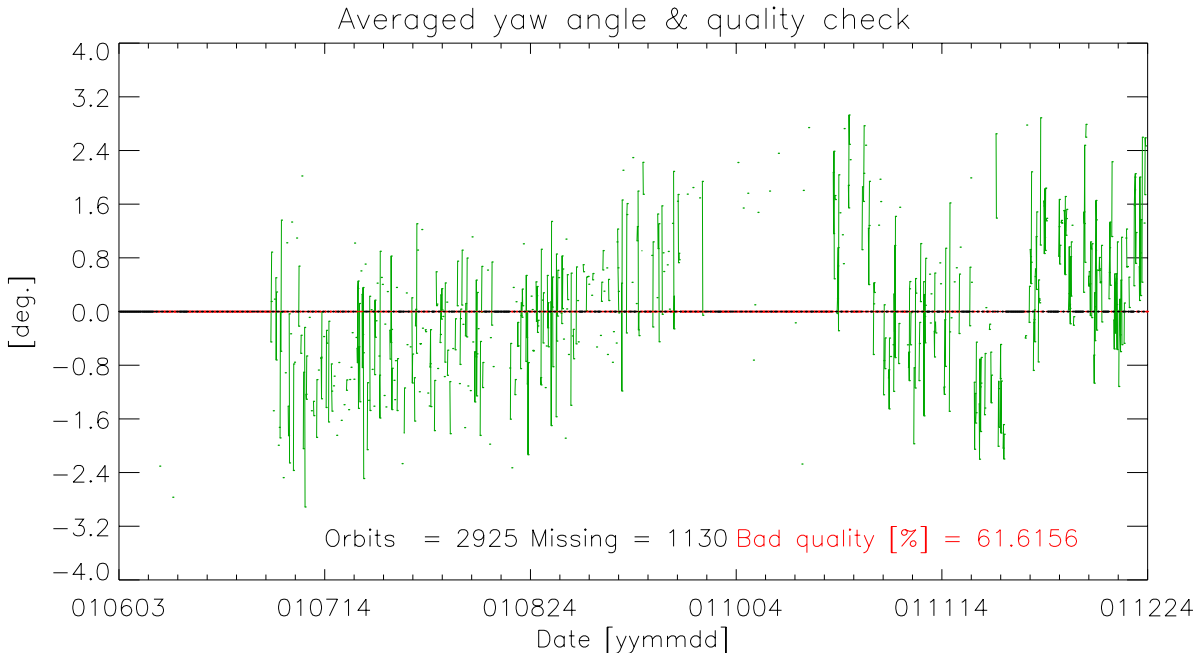

FIGURE 30. Averaged yaw error angle since June 2001

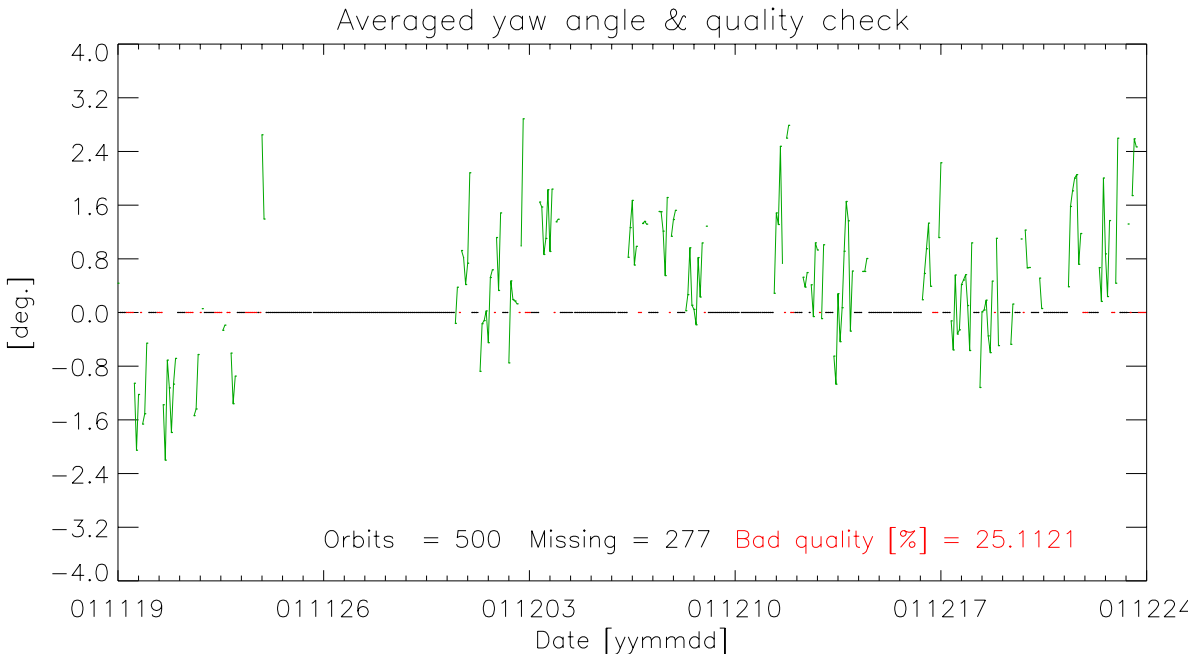

FIGURE 31. Averaged yaw error angle for cycle 69